Supramolecular Chemistry
Publication details, including instructions for authors and subscription information:
http://www.informaworld.com/smpp/title~content=t713649759

Supramolecular architectures of functionalized tetraphenylmetalloporphyrins in crystalline solids. Studies of the 4-methoxyphenyl, 4-hydroxyphenyl and 4-chlorophenyl derivatives

Israel Goldberg[ab]; Helena Krupitsky[ab]; Zafra Stein[ab]; Yu Hsiou[ab]; Charles E. Strouse[ab]
[a] School of Chemistry, Sackler Faculty of Exact Sciences, Tel-Aviv University, Ramat-Aviv, Israel [b] Department of Chemistry and Biochemistry, University of California, Los Angeles, CA, U.S.A.

To cite this Article Goldberg, Israel , Krupitsky, Helena , Stein, Zafra , Hsiou, Yu and Strouse, Charles E.(1994) 'Supramolecular architectures of functionalized tetraphenylmetalloporphyrins in crystalline solids. Studies of the 4-methoxyphenyl, 4-hydroxyphenyl and 4-chlorophenyl derivatives', Supramolecular Chemistry, 4: 3, 203 — 221
To link to this Article: DOI: 10.1080/10610279408029473
URL: http://dx.doi.org/10.1080/10610279408029473

SUPRAMOLECULAR CHEMISTRY, Vol. 4, pp. 203–221
Reprints available directly from the publisher
Photocopying permitted by license only

Supramolecular architectures of functionalized tetraphenylmetalloporphyrins in crystalline solids. Studies of the 4-methoxyphenyl, 4-hydroxyphenyl and 4-chlorophenyl derivatives

ISRAEL GOLDBERG*, HELENA KRUPITSKY, ZAFRA STEIN, YU HSIOU and CHARLES E. STROUSE*

School of Chemistry, Sackler Faculty of Exact Sciences, Tel-Aviv University, 69978 Ramat-Aviv, Israel, Department of Chemistry and Biochemistry, University of California, Los Angeles, CA 90024-1569, U.S.A.

Keywords: Aggregation modes of, crystalline complexes of metalloporphyrins, functionalized tetraphenylporphyrins.

(Received March 24, 1994)

A series of new "inclusion" materials based on tetra-4-methoxyphenyl, tetra-4-hydroxyphenyl and tetra-4-chlorophenyl derivatives of the metalloporphyrin system, in combination with a wide variety of guest molecules and ligands, have been prepared, and their structural systematics analysed. Crystallographic investigations have confirmed that the supramolecular arrangement of the hydroxyphenylporphyrin species is dominated by interporphyrin directional hydrogen-bonding interactions, and consists of continuous networks of strongly coordinated entities with varying degrees of cross-linking and rigidity. Guest molecules can be absorbed in these solids in distinctly defined sites of the lattice: in the small interhost cages of fixed size between adjacent intercoordinated porphyrin hosts, or in extended one-dimensional channels formed between the hydrogen bonded host arrays running parallel or perpendicular to the porphyrin plane. For polar ligands with strong nucleophiles, their potential coordination to the metal center provides an additional recognition factor. The stacking mode (offset geometry or overlapping) of the host metalloporphyrin arrays is also affected by the nature of the incorporated guest/ligand. Materials based on the chloro-substituted porphyrins were found to form similarly networked structural modes, influenced by the molecular shape as well as by halogen-halogen noncovalent interactions. Formation of a polar tubular intermolecular architecture capable of aligning organic dipolar guest molecule in the crystal bulk has also been demonstrated. The methoxy-substituted materials form clathrate-type structures characterized by dense layered arrangement of the porphyrin building blocks in two-dimensions. The various structural features directing the observed modes of the supramolecular architecture, and affecting the host structure as well as the guest mobility in it, are discussed.

*Corresponding author.

INTRODUCTION

Microporous molecular materials with nanometer dimension channel and cage type architectures represent a continuously challenging frontier of solid state science. Most of their applications are based on the ability of the open crystalline structures to selectively incorporate other species within the void spaces on a molecular scale, and to modify the physical and chemical characteristics of the 'guests'. This potential has led to the development of several strategies for the designed construction of 'host' building blocks and their structure-enforced supramolecular assemblies. Such materials have become particularly useful in modern studies of molecular devices, biological molecular recognition and drug design.

Earlier investigations have elucidated the structural systematics of the host lattice and the remarkable versatility of tetraphenylmetalloporphyrin complexes as formers of crystalline heteromolecular materials [1–4]. The regularity of these structures, irrespective of the host/guest constitution, reflects the high degree to which the crystal packing is dominated by porphyrin-porphyrin dispersion forces. The feasibility of several applications of the solid porphyrins relating to molecular recognition and chemical separations, matrix isolation, and matrix dilution of paramagnetic compounds have been demonstrated. The unique modes of aggregation of various porphyrin and tetraarylporphyrin compounds in thin layers

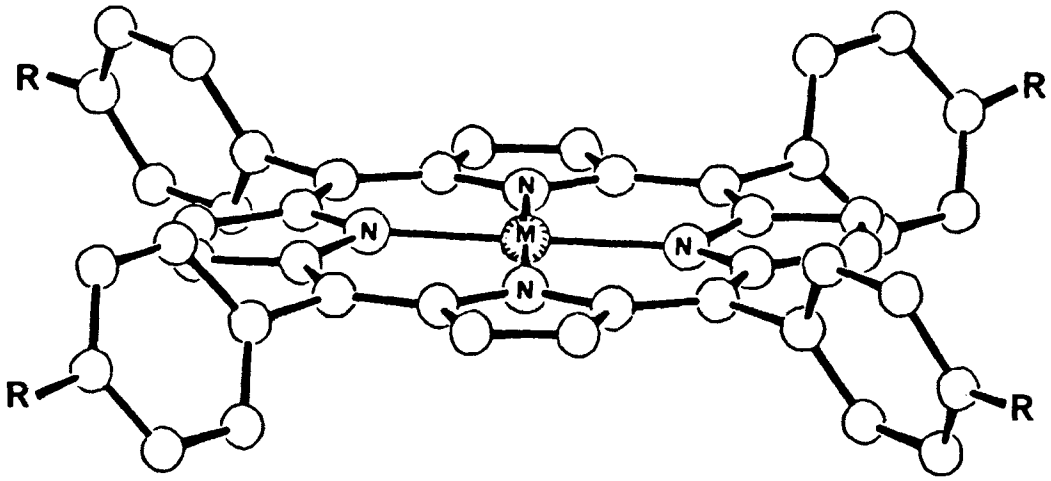

Figure 1 The porphyrin host framework. Structural modifications: M = Co, Cu and Zn; R = OCH_3, OH and Cl.

[5], as well as in the solution [6–8] have also been studied in recent years.

In order to control better the modes of intermolecular aggregation in the solid state, polar sensor groups can be introduced into the molecular framework of the tetraphenylmetalloporphyrin derivative (Fig. 1). [9] Chemical substitution on the porphyrin phenyl groups provides an almost unlimited variety of 'building blocks' for the construction of supramolecular assemblies. The nature of the substituent can be used to control the rigidity of such an assembly. The current approach is based on functionalization of the rigid porphyrin molecular framework with polarized aryl groups, which may then be used to link the host molecules into a fixed one-, two- or three-dimensional polymeric patterns. Controlled variation of the microstructure in the resulting solids, and consequently of their structure-dependent properties, will be effected primarily by changing the type (and size) of the sensor group and its disposition in the porphyrin molecule. In closely related studies carried out by others, similarly functionalized porphyrins have successfully been used to develop simple chemical models of self-assembly in solution based on noncovalent interactions [10], and also to prepare molecular compounds with tailored quadratic nonlinear optical properties [11].

We report here the structure and crystal inclusion properties of several metalloporphyrin compounds that have various substituents attached to the aryl groups, including Co(II)- and Zn(II)-tetra-(4-methoxyphenyl)porphyrin (**1** and **2**, respectively), Cu(II)- and Zn(II)-tetra-(4-hydroxyphenyl)porphyrin (**3** and **4**, respectively), and Zn(II)-tetra-(4-chlorophenyl)porphyrin (**5**). A comprehensive evaluation of the structural patterns observed in a large series of new crystalline materials is presented below [9]. Correlation of the structural features with the substitution type of the host compounds is also discussed. Structural studies of the 3,5-di-*t*-butyl-4-hydroxyphenyl derivative of various metalloporphyrins have been reported earlier [12,13].

EXPERIMENTAL SECTION

Preparation of the Crystalline Compounds. Starting materials were purchased from Midcentury (porphyrins), Aldrich and Fluka (all other reagents). The complexed crystalline solids were obtained by recrystallization of the corresponding porphyrin derivative from a minimum amount of the respective guest liquid. Common solvents (such as: methanol, glacial acetic acid, ethyl acetate) were used is some cases to control solubility of the porphyrin constituent. Suitable crystals for X-ray diffraction were prepared in various ways, including slow cooling, solvent diffusion, and solvent evaporation in an open air for long periods of time (several weeks). List and composition of the crystalline compounds subjected to a detailed structural investigation are given in Table 1. Crystals of compound **19** were grown from a 1:1:1:1 solvent mixture of toluene, *o*-xylene, *m*-xylene and *p*-xylene, but the actual content of the individual components in the crystal could not be determined; for simplicity the guest component in **19** is represented in Table 1 by toluene alone.

Data collection. The X-ray diffraction experiments were carried on automated CAD4 (at Tel-Aviv University), Huber and Picker (at UCLA) diffractometers equipped with a graphite monochromator. Intensity data were collected by the ω-2θ can mode with a constant speed (1.5, 3.0 or 4.5 deg/min, according to the diffraction power of the analyzed crystal), using Mo-Kα (λ=0.7107 Å) radiation. Some of the analyzed crystals were covered by a thin layer of epoxy resin to prevent desorption of the guest component from the porphyrin lattice during data collection. Possible deterioration of the crystals during the measurements was tested by periodic detection of the intensities of three standard reflections from different zones of the reciprocal space. For most compounds it was found negligible; the standard intensities of **6**, **7**, **12** and **13** exhibited a slight linear decrease (of about 7%, 10%, 3% and 3%, respectively)

Table 1 *List of materials subjected to crystal structure analysis.*

Compound	*host*	*ligand/guest*	*formula, and host:guest ratio in crystals*
6	**1**	benzyl alcohol	$C_{48}H_{36}N_4O_4Co.C_7H_8O$ (1:1)
7	**1**	chlorobenzene	$C_{48}H_{36}N_4O_4Co.C_6H_5Cl$ (1:1)
8	**2**	*m*-cresol	$C_{48}H_{36}N_4O_4Zn.C_7H_8O$ (1:1)
9	**2**	phenol, water	$C_{48}H_{36}N_4O_4Zn.C_6H_6O.H_2O$ (1:1:1)
10	**2**	*o*-hydroxyacetophenone	$C_{48}H_{36}N_4O_4Zn.C_8H_8O_2$ (1:2)
11	**4**	*p*-cresol, water	$C_{44}H_{28}N_4O_4Zn.C_7H_8O.H_2O$ (1:2:2)
12	**4**	ethylacetate, DMF, water	$C_{44}H_{28}N_4O_4Zn.C_4H_8O_2.C_3H_7NO.H_2O$ (3:2:2:13)
13	**4**	phenol, water	$C_{44}H_{28}N_4O_4Zn.C_6H_6O.H_2O$ (1:2:2)
14	**4**	benzyl acetate, water	$C_{44}H_{28}N_4O_4Zn.C_9H_{10}O_2.H_2O$ (1:2:1)
15	**4**	benzaldehyde, water	$C_{44}H_{28}N_4O_4Zn.C_7H_6O.H_2O$ (1:2:1)
16	**3**	acetophenone	$C_{44}H_{28}N_4O_4Cu.C_8H_8O$ (1:4)
17	**4**	*o*-xylene, methanol	$C_{44}H_{28}N_4O_4Zn.C_8H_{10}.CH_4O$ (1:2:4)
18	**4**	guaiacol	$C_{44}H_{28}N_4O_4Zn.C_7H_8O_2$ (1:5)
19	**4**	toluene	$C_{44}H_{28}N_4O_4Zn.C_7H_8$ (1:3)
20	**5**	methyl phenylacetate	$C_{44}H_{24}Cl_4N_4Zn.C_9H_{10}O_2$ (1:1)
21	**5**	mesitylene, water	$C_{44}H_{24}Cl_4N_4Zn.C_9H_{12}.H_2O$ (1:1:0.7)
22	**5**	ethylbenzoate	$C_{44}H_{24}Cl_4N_4Zn.C_9H_{10}O_2$ (1:1)
23	**5**	acetophenone	$C_{44}H_{24}Cl_4N_4Zn.C_8H_8O$ (1:2)
24	**5**	*nitrobenzene*	$C_{44}H_{24}Cl_4N_4Zn.C_6H_5NO_2$ (1:1)

over the entire experiment, which required an appropriate correction of these sets of data. Initially, no corrections for absorption (the absorption coefficients being still relatively small) and secondary extinction effects were applied. Repeated calculations were performed with data sets empirically corrected for absorption, but did not yield a significant improvement of the results. The cell constants and pertinent details of the experimental conditions are summarized in Table 2.

Structure Analysis and Refinement. The crystal structures were solved by a combination of direct methods and Fourier techniques (MULTAN 80 and SHELXS 86). [14,15] Their refinements were carried out by large-block least-squares (SHELX 76) [16], including the positional and anisotropic thermal parameters of the non-hydrogen atoms. Final calculations were based only on those observations that satisfied the conditions $I > 2\sigma(I)$ in **5** and **15** and $I > 3\sigma(I)$ in the other structures.

Standard crystallographic refinements of compounds **6–24** converged at reasonably low *R*-values (Table 2), allowing a reliable description of the atomic parameters and of the intermolecular interaction scheme. However, guest components residing in interporphyrin voids, which are not coordinated to the metalloporphyrin ring system, or to the polar sensor groups in these structures, as well as guests located in the lattice on elements of crystallographic symmetry (see below), often exhibit structural disorder. Consequently, they were included in the calculations with constrained geometries and isotropic thermal parameters only to avoid unreliable distortions of covalent parameters. In order to maximize the data-to-parameters ratio the porphyrin phenyls in some of the compounds were also refined as regular hexagons; furthermore, for four structures **12**, **13**, **17** and **19** intensity data were collected at 145K. Due to a particularly small number of significant observations obtained from the tiny crystals of compound **15**, anisotropic thermal motion parameters were assigned in this case only to the heavier Zn ion, while the light C, N and O atoms were refined isotropically. Similar difficulties in the refinement of the composite porphyrin structures have been experienced in the related studies as well [2,12]. Most hydrogen atoms were introduced into the structure factor computations in calculated positions, the methyl substituents being treated as rigid groups. Approximate positions of some of the hydroxy H-atoms could be found directly in difference-Fourier maps. The final difference electron-density maps (all, except in **17**, with peaks and troughs of <1.0 e.Å^{-3}) of the nineteen structures showed no indication of incorrectly placed or missing atoms.

The space symmetry of the various packing motifs, and thus the intensity distribution in the corresponding diffraction patterns, is determined primarily by the spatial arrangement of the large porphyrin moieties. The experimental data are often not sensitive enough to reliably detect incommensurate symmetries (if present) of the host and the much smaller guest/solvate component. As a result, some of the structural models chosen to optimally fit the diffraction data in the refinement calculations contain asymmetrically shaped solvate species constrained to lie on, and be disordered about, crystallographic elements of symmetry (e.g., inversion center, twofold rotation axis or mirror plane).

The final atomic coordinates, lists of the anisotropic thermal parameters, as well as bond lengths and bond angles have been submitted as Supplementary Material and deposited at the Cambridge Crystallographic Data Centre.

RESULTS

Structures of the M(II)-tetra-(4-methoxyphenyl)porphyrins. The crystal structures of **6**, **7** and **8** are charac-

Table 2 *Summary of crystal data and experimental parameters.*

Compound	*6*	*7*	*8*	*9*	*10*	*11*	*12*[c]	*13*[c]	*14*
FW[a]	899.9	904.3	906.4	910.3	1070.5	994.4	2782.9	966.4	1060.5
Space group	*Cc*	$P2_1/c$	$P2_1/c$	C2/c	$A\bar{1}$	$P2_1/c$	$P\bar{1}$	$P2_1/c$	$P\bar{1}$
Z	4	2	2	4	2	4	1	4	2
a, Å	31.326(11)	14.394(3)	14.672(9)	19.909(3)	9.217(1)	9.776(1)	11.948(2)	20.140(1)	13.586(2)
b, Å	9.683(6)	9.675(6)	9.675(6)	9.446(1)	14.770(1)	19.469(1)	14.398(2)	10.734(1)	14.662(13)
c, Å	15.702(2)	15.624(3)	15.713(7)	23.599(3)	19.663(2)	25.243(1)	21.300(4)	21.381(1)	15.170(7)
α, deg	90.0	90.0	90.0	90.0	91.10(1)	90.0	88.13(1)	90.0	82.26(5)
β, deg	112.18(2)	99.11(2)	98.53(2)	93.61(1)	101.07(1)	91.29(1)	75.03(1)	98.40(1)	67.20(3)
γ, deg	90.0	90.0	90.0	90.0	91.50(1)	90.0	65.91(1)	90.0	66.84(5)
V, Å^3	4410.4	2148.4	2205.8	4429.2	2525.4	4803.2	3220.5	4572.8	2560.7
D_c, g cm^{-3}	1.35	1.40	1.36	1.37	1.35	1.38	1.43	1.40	1.38
F(000)	1876	938	944	1896	1116	2072	1452	2008	1104
μ, cm^{-1}	4.40	5.12	6.22	6.21	5.37	5.82	6.49	6.09	5.51
2θ limits, deg	50	46	42	46	46	46	46	50	50
N(unique)	4319	3332	2042	2754	3290	5664	7376	6851	5951
N(obs)[b]	3131	2118	1131	2093	2575	3807	4562	4741	2953
R_F	0.090	0.066	0.074	0.041	0.040	0.044	0.057	0.041	0.069
*w*R	0.087	0.067	0.072	0.044	0.042	0.047	0.055	0.041	0.067
$\lvert\Delta\rho\rvert_{max}$	0.64	0.62	0.58	0.25	0.31	0.29	0.49	0.31	0.52

[a]Formula weights refer to the molecular entities described in Table 1.
[b]For compounds **6** and **15** $I > 2\sigma(I)$, otherwise $I>3\sigma(I)$.
[c]Data collected at 145 K, otherwise at room temperature (*ca* 278 K).

Compound	*15*	*16*	*17*[c]	*18*	*19*[c]	*20*	*21*	*22*	*23*	*24*
FW[a]	972.4	1220.9	1082.6	1362.8	1018.4	966.1	948.7	966.1	1056.2	939.0
Space group	$Pmc2_1$	$P\bar{1}$	$P2_1/n$	$P\bar{1}$	$I2/m$	$P\bar{1}$	$C2/c$	$P6_2$	$P\bar{1}$	$P2_1$
Z	4	1	2	1	2	2	8	3	1	2
a, Å	15.538(3)	11.651(3)	14.666(1)	6.549(2)	6.509(1)	9.782(3)	17.203(3)	16.845(3)	8.239(5)	15.439(6)
b, Å	15.175(7)	11.720(5)	17.875(2)	14.450(2)	21.103(4)	14.952(12)	28.938(3)	16.845	12.104(3)	9.387(2)
c, Å	19.934(5)	13.972(3)	12.048(1)	18.843(5)	19.754(3)	16.827(5)	17.640(3)	13.837(2)	13.580(9)	14.323(11)
α, deg	90.0	69.54(3)	90.0	104.77(1)	90.0	111.64(4)	90.0	90.0	78.49(3)	90.0
β, deg	90.0	79.76(3)	61.99(1)	90.16(2)	90.23(1)	101.80(2)	109.58(2)	90.0	84.06(5)	98.22(3)
γ, deg	90.0	59.69(4)	90.0	99.41(2)	90.0	98.96(4)	90.0	120.0	70.40(3)	90.0
V, Å^3	4700.2	1543.2	2788.6	1699.2	2713.4	2165.8	8273.8	3400.3	1249.2	2054.4
D_c, g cm^{-3}	1.37	1.31	1.29	1.33	1.42	1.48	1.52	1.41	1.40	1.52
F(000)	2016	637	1140	712	1064	988	3840	1482	542	956
μ, cm^{-1}	5.92	4.13	5.06	4.36	5.82	8.76	9.11	8.37	7.65	9.21
2θ limits, deg	50	50	50	50	46	50	50	46	50	50
N(unique)	2855	4897	5349	5301	1837	6965	5696	1645	4098	3316
N(obs)	1311	3000	2316	3049	1519	4880	2316	1188	3210	1852
R_F	0.108	0.095	0.062	0.082	0.061	0.055	0.070	0.064	0.041	0.058
*w*R	0.094	0.095	0.067	0.081	0.062	0.056	0.070	0.048	0.043	0.059
$\lvert\Delta\rho\rvert_{max}$	0.78	0.58	1.05	0.56	0.54	0.56	0.65	0.58	0.33	0.55

terized by a very similar arrangement of the porphyrin building blocks. It consists of tightly packed two-dimensional layers of the porphyrin molecules, in which the latter are stacked in an offset manner, the mean planes of the porphyrin cores being roughly parallel to one another and roughly perpendicular to the layer (Fig. 2a,b). There are no guest/solvent molecules within these layers. In this offset stacked geometry, each porphyrin core is sandwiched between four 4-methoxyphenyl arms of the adjacent species. The remaining methoxyphenyl groups extend into the layer interspace. The periodicity of this two-dimensional arrangement can be conveniently described by a rectangular pseudo-centered cell of approximate dimensions of 9.7A × 15.6–15.7Å (Fig. 2a,b). Stacking of these layers in the third dimension is less effective, as the perpendicularly oriented methoxyphenyl arms of one layer cannot penetrate into the neighboring layers. Introduction of guest molecules into the inter-layer voids stabilizes the structure of the condensed solid phase. Figures 3a and 3b illustrate the crystal structures of **6** and **7**; the interlayer packing in **8** is isomorphous to that in **7**. Lacking specific interaction with the surrounding molecules, the guest components are disordered in the crystalline lattice. Structure **6** is noncentrosymmetric, the methoxy substituents being asymmetrically oriented with respect to the porphyrin core. The benzyl alcohol species incorporated in it are both translationally and orientationally disordered, their position being thus poorly defined. The structures of **7** and **8** are centrosymmetric with the metalloporphyrin molecules located on centers of inversion. In both compounds the guest constituents (chlorobenzene and *m*-cresol, respectively) are also located on and orientationally disordered about inversion centers. Evidently, the interlayer spacing and rel-

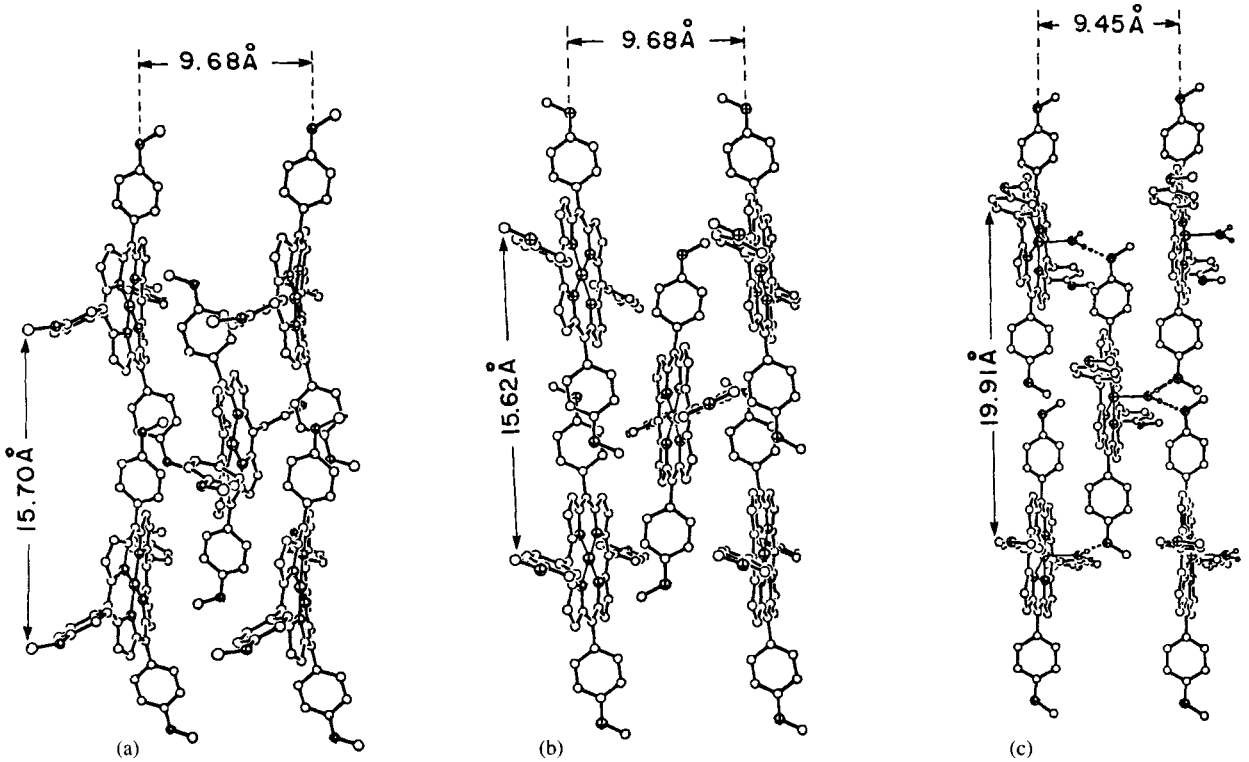

Figure 2 Illustration of the tight "square-centered" layered arrangement of the methoxy-substituted porphyrin species in compounds: (a) **6** (projection on the **bc** plane), (b) **7** (projection on the **bc** plane, and (c) **9** (projection on the **ab** plane).

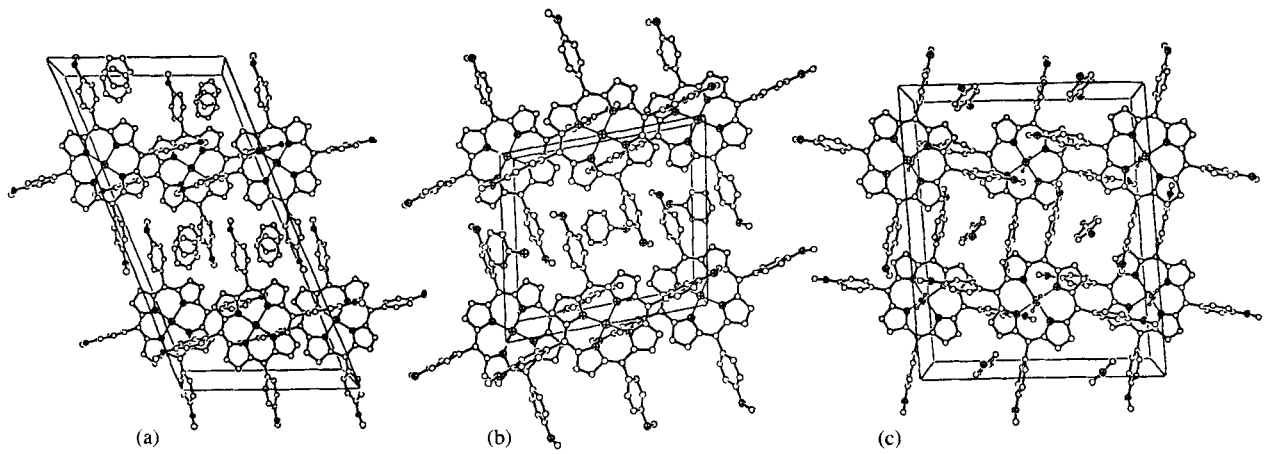

Figure 3 Crystal packing modes observed in the methoxy substituted porphyrin materials (viewed down the short **b**-axis of the corresponding crystals). (a) Compound **6**; the translationally disordered benzyl alcohol solvent is represented by two partially overlapping hexagons. (b) Compound **7**; only one orientation of the chlorobenzene is shown. (c) Compound **9**; the "disubstituted" phenyl guest moiety shown represents a phenol molecule located on, and disordered about, crystallographic inversion centers.

ative inclination are the most variable parameters of the crystalline lattice, being sensitive to the overall size and shape of the incorporated guest moiety. The periodic translation along the **a**-axis in the two nearly isomorphous structures varies, for example, from 14.39Å in **7** to 14.67Å in **8**, reflecting on the different shapes of the chlorobenzene and *m*-cresol guests. Additional crystalline compounds of porphyrin **1** with other guest components have been prepared. A 1:1 incorporation of ethylbenzoate (monoclinic-C, a=31.084, b=9.624, c=15.634Å, β = 111.4°) and of guaiacol (monoclinic-C, a = 31.657, b = 9.618, c = 15.772A, β = 112.36°) yields isostructural arrangements to that in **6**, while incorporation of *o*-chlorophenol (monoclinic-P, a = 14.427, b = 9.687, c = 15.553Å, β = 99.23°) forms a structure isomorphous with that in **7**. The above data confirm that in the two structure types, the **a**-dimension (interlayer spacing) is subjected to largest variation.

An interesting modification occurs when the crystalline materials are prepared from wet (water-containing) solvents. This is illustrated by the structure of compound **9** which represents a ternary complex of porphyrin-**2**, phenol and water. The small molecule of water is ligated to the central metal ion (both are located on an axis of twofold rotational symmetry) producing a five-coordinate complex. Evidently, presence of the additional ligand strengthens the layered arrangement of the porphyrin moieties, preserving the offset stacked geometry. In order to accommodate the additional ligand and to utilize its hydrogen-bonding capacity, the layers expand considerably in the direction corresponding to the longer dimension of the unit cell of the layer. This dimension is increased by about 4Å with respect to the former examples, to 19.9 Å. This lowers the steric hindrance between the methoxy fragments and the neighboring porphyrins, allowing a slight contraction of the two-dimensional layer along a direction perpendicular to the porphyrin plane (even in the presence of the additional water molecule; Fig. 2c). The resulting structure reveals that all porphyrin moieties in a given layer are now strongly cross-linked by the water moiety. Each molecule of water, while ligating through its oxygen to the metal center of one porphyrin at 2.20Å, donates its two protons to the methoxy groups of adjacent porphyrins on opposite sides (at an OH•••O distance of 2.98Å). The Zn atom is displaced from the mean plane of the four N atoms by 0.28 Å. The phenol molecules are accommodated in voids between neighboring layers of the H-bonded sheets, being located on and disordered about crystallographic centers of inversion. As in structures **6–8**, they fill the interlayer pores created between the methoxyphenyl fragments which point outward from the individual layers, without specific interactions with their environment (Fig. 3). A similar structure is formed upon incorporation of *m*-xylene from a wet solvent [2]. In that material, the aprotic *m*-xylene guest ligand is accommodated within the interlayer pores in much the same manner as the protic phenol constituent in **9**.

With a larger guest component containing a strong carbonyl nucleophile, such as *o*-hydroxyacetophenone, host **2** forms a 1:2 six-coordinate complex. Here, the Zn(II) ion is located on an inversion center in a distorted octahedral environment, being linked strongly to the N-atoms of the porphyrin core at 2.04–2.05Å, and approached from above and below by two carbonyl oxygens of the weakly coordinated guest component at 2.72 Å. Incorporation of two guest moieties per porphyrin at the apical coordination sites of the metal ion requires a considerable expansion of the stacked arrangement of the metalloporphyrin derivatives. However, as shown in Fig. 4, the "pseudo-square-centered" mode of interporphyrin stacking is preserved, only now the *o*-hydroxyacetophenone ligands (instead of the methoxyphenyl fragments) are inserted in pairs between porphyrins displaced by a unit-cell translation. The increased distance between adjacent porphyrinic entities within a given layer allows a considerably more effective interlayer approach and interpenetration of the methoxyphenyl groups, without formation of open voids in between (Fig. 4).

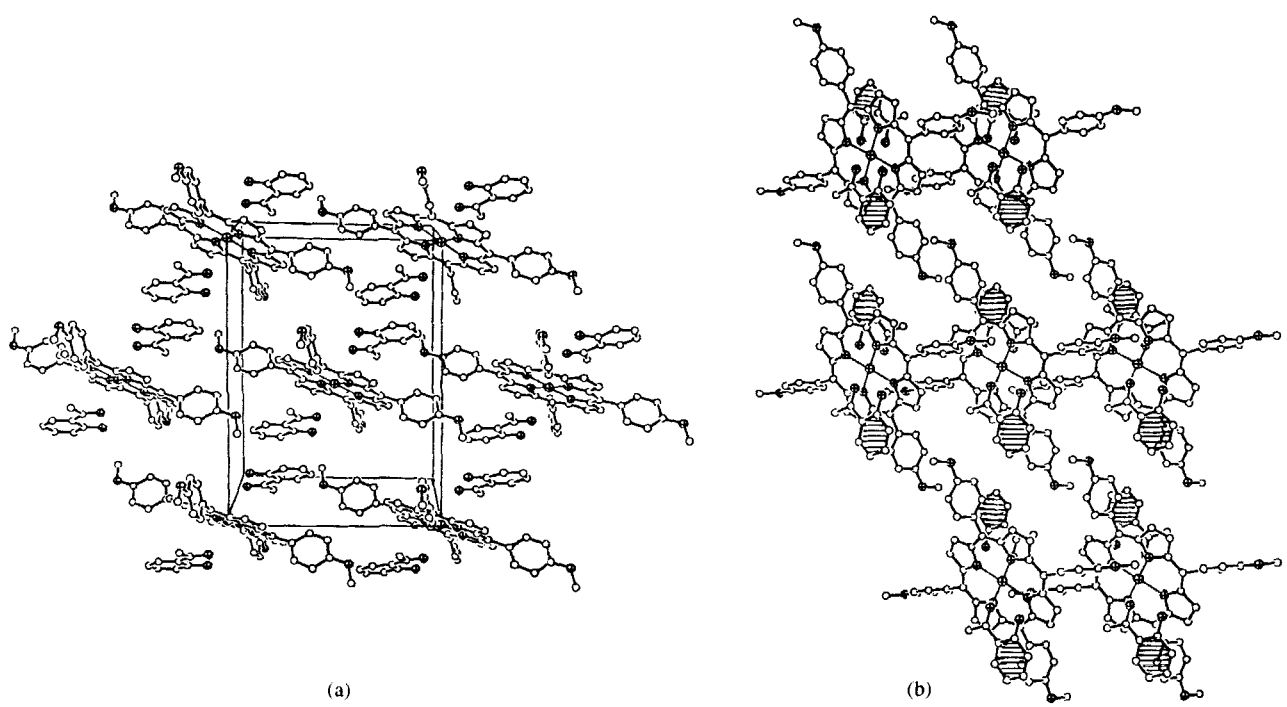

Figure 4 The crystal structure of **10**. Two views (a) approximately down **a** and (b) approximately down **c**, showing corrugated sheets of the porphyrin moiety interspaced by the *o*-hydroxyacetophenone ligands; the latter are shaded in (b).

Inspection of the crystallographic data reveals some additional relevant details. In **9** the tight packing of the coordinated methoxyphenyl groups within the layers, as opposed to the relatively loose packing of the uncoordinated arms, is clearly reflected in the correspondingly small and large parameters of thermal motion of the two perpendicularly oriented groups. Consistent results are obtained also in the crystallographic refinements of structures **6–8**. The steric hindrance caused by the in-layer OMe groups in structures of the four-coordinate metalloporphyrins **6–8** may be the main reason for the observed deviations from coplanarity of adjacent porphyrin cores within a given layer (the non-overlapping porphyrin molecules are related to each other by the screw/glide symmetry) in the different structures. Coordination distances of the larger Zn(II) ion to the porphyrin N-sites in **2** are all within 2.04–2.06 Å, including those in the 5-coordinated compound in which the metal ion deviates slightly from the plane of the porphyrin core. Average coordination distances of the smaller Co(II) ion to N in **1** are shorter, near 1.96 Å. In the latter case deformations of the porphyrin core from planarity ("ruffling") tend to occur more frequently [17].

Structures of the M(II)-tetra-(4-hydroxyphenyl)porphyrins. Crystals of these materials exhibit an even larger variety of structural modes with different degrees of complexity. The intermolecular arrangement in **11** can be best described in the following manner. Adjacent metalloporphyrins displaced along **b** are linked to each other by hydrogen bonds between their peripheral OH functions. Two *trans*-related hydroxyphenyl groups of every porphyrin moiety are involved in these interactions, thus forming continuous arrays of hydrogen-bonded molecules in this direction. The one-dimensional chains are stacked one on top of the other in a partly overlapping manner along **a** to yield layered zones of the host molecules at $z = 0$ and $z = 0.5$. The incorporated *p*-cresol and water species are accommodated between these zones. They hydrogen bond to one another and to the porphyrin OH groups. Consequently, they provide cross-linking bridges between adjacent porphyrin layers displaced by c/2 (Fig. 5). The metal center of the porphyrin is four-coordinate. However, the porphyrin core is significantly deformed from planarity (assuming the "sad" form [1]) due to considerable steric hindrance between the aryl substituents and the porphyrin core of the overlapping moieties.

Crystals of **12** are characterized by a complex stoichiometry (Table 1). The asymmetric unit of this structure contains one porphyrin molecule at a general site (A) and another located on an inversion center (B). The Zn atom in the former is displaced from the least-squares plane of the four nitrogen atoms by 0.16 Å and is coordinated to an axially positioned water, at 2.20 Å, producing a 5-coordinate complex. In the latter case two molecules of dimethylformamide lie close to the porphyrin core across the center of inversion. The Zn-ion in this species deviates significantly (0.31 Å) from the por-

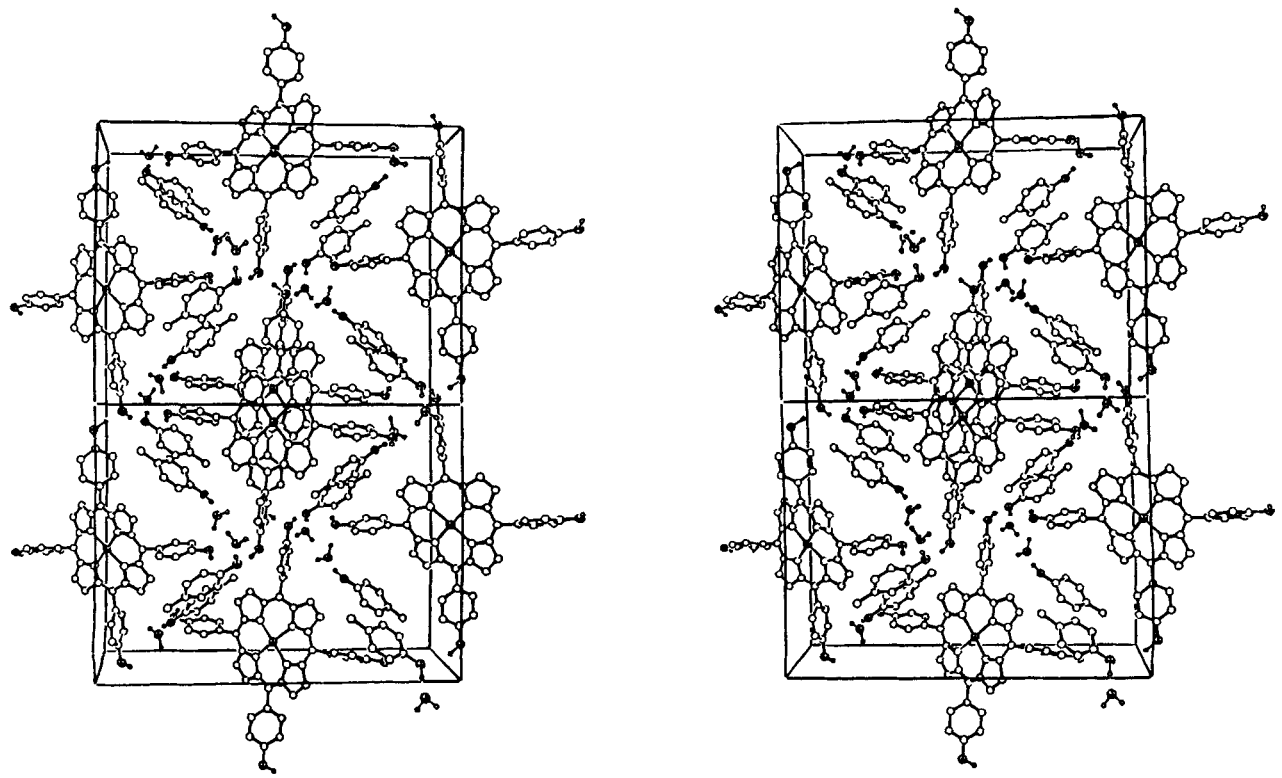

Figure 5 Stereoview of the crystal structure of **11**, down the shortest **a**-axis. Two unit cells are shown to illustrate better the various aspects of the intermolecular interaction.

phyrin plane, exhibiting a twofold disorder about the inversion. This suggests that the metal center is preferentially ligated by one of the two DMF species (at 2.41 Å to its carbonyl oxygen) to assume a pentagonal coordination. The porphyrins at the two sites are nearly perpendicular to one another. Similarly to previous observations in **9**, the metal-coordinated water of porphyrin-A links effectively through hydrogen bonds to the hydroxyl ends of two neighboring porphyrins of type B. Thus in the resulting structure (Fig. 6), each porphyrin-B bridges between two centrosymmetrically related moieties of porphyrin-A, yielding a continuous one-dimensional pattern of hydrogen bonded molecular frameworks along the **b+c** direction. These chains are stacked tightly in layers parallel to the (**bc**) plane of the unit-cell. Molecules of ethyl acetate are also H-bonded to the metal-ligated water, filling the intermolecular space within each such layer. Four hydroxyphenyl groups of porphyrin-A and two hydroxyphenyl arms of porphyrin-B turn outward, their polar ends being surrounded by additional molecules of water. The aqueous zone interfaces between adjacent porphyrin layers, provides coordination shell to the six hydroxyphenyl fragments, and stabilizes the entire structure by H-linking the neighboring zones of the porphyrin moieties. Distortion from planarity of the ring system of porphyrin-A is evident. Most probably it occurs due to close steric interactions between the uncoordinated faces of adjacent porphyrin species related to one another in a back-to-back manner. This structure is unique in the sense that it contains in the same crystal two different 5-coordinate porphyrins.

The metal center in **13** is also five-coordinate; to the four N-sites and to an apical water (at 2.21 Å); it is displaced from the mean plane of the four nitrogen atoms by 0.28 Å. In this structure (Fig. 7), the porphyrin molecules are hydrogen bonded to one another across the centers of inversion. This association of the centrosymmetrically related fragments involves two *cis*-related hydroxyphenyl arms of two different porphyrin rings, yielding continuous rows of hydrogen bonded metalloporphyrin moieties. Neighboring rows, related by the screw/glide symmetry and aligned in nearly perpendicular directions, are further linked to each other by hydrogen bonds between the metal-coordinated water of one array and two of the peripheral hydroxy groups of adjacent arrays. The phenol moieties and an additional water accommodate the interporphyrin pores. These guest molecules also form an H-bonded cluster, which is linked at one end to the metal-coordinated water.

Hydrogen-bond assisted assembly of the tetra-4-hydroxyphenyl derivatives of metalloporphyrin through the *cis*-related hydroxyphenyl fragments of adjacent moieties is also observed in many other structures (see below). In such an arrangement, simple molecular species

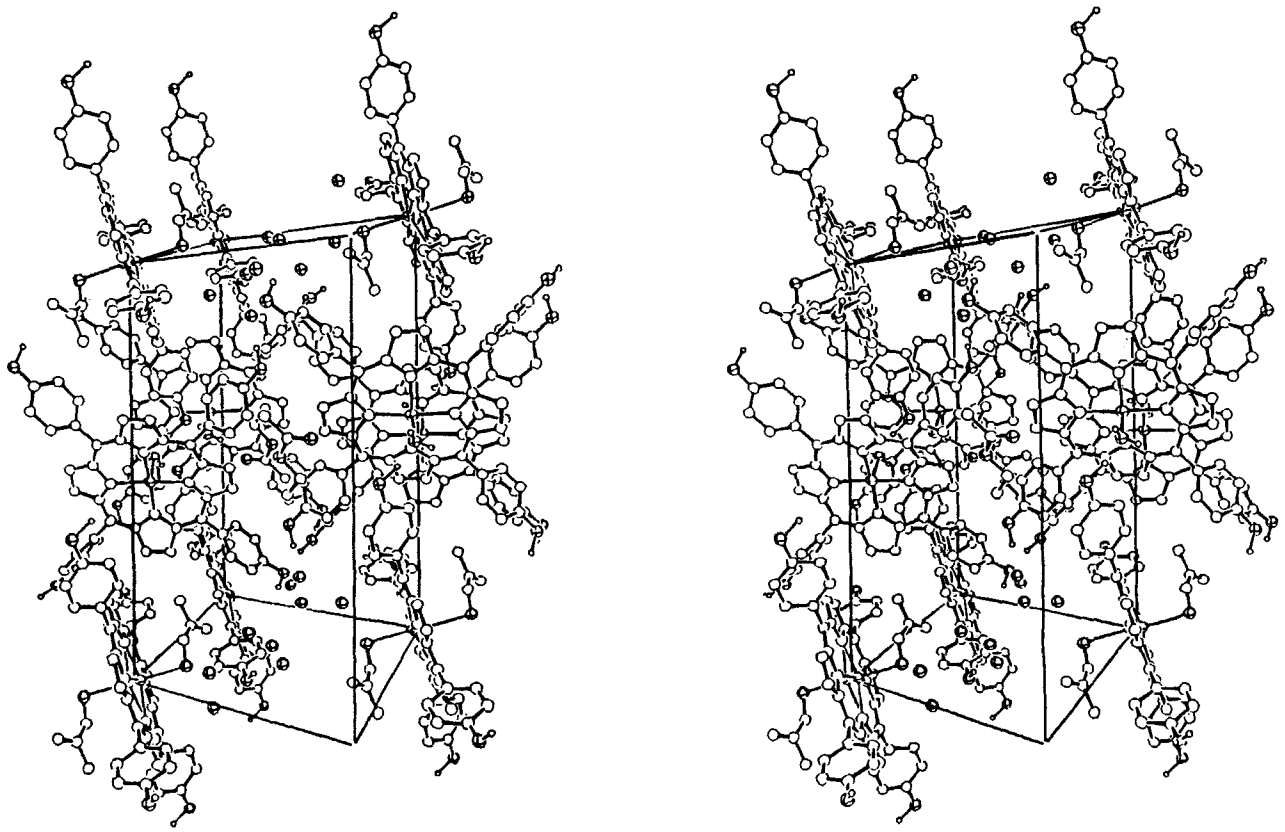

Figure 6 Stereoview of the crystal structure of **12**, illustrating the complexity of the intermolecular organization in this solid. The water-coordinated porphyrin-A located at a general site is roughly parallel to the projection of this drawing; porphyrin-B located on an inversion center is seen edge on.

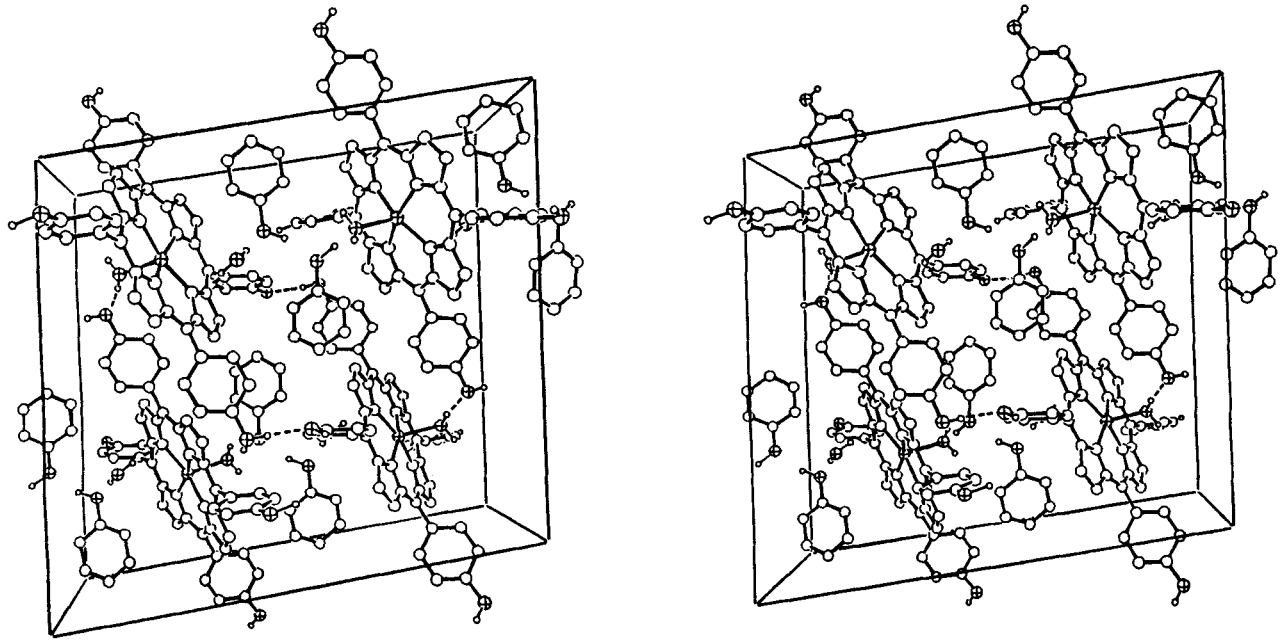

Figure 7 Stereoview of the crystal structure of **13** down the **b**-axis. The interporphyrin association through hydrogen bonds between the hydroxyphenyl residues, and those involving the metal ligating water, is marked by dashed lines.

can be readily occluded into the interporphyrin pores thus formed. This is demonstrated by the following structures involving porphyrins **3** and **4**, in which water plays a less significant role, or which had been crystallized from anhydrous solvents.

The crystal structure of **14** can be best described as consisting of two dimensional layers of metalloporphyrin moieties H-linked to one another in both directions by the peripheral OH groups. The metalloporphyrin is 5-coordinate, including the benzyl acetate ligand at the apical position with its carbonyl oxygen 2.40 Å distant from the Zn-ion. In a given layer two intermolecular pores are associated with each porphyrin moiety (Fig. 8a). The centrosymmetrically related layered assemblies are positioned one on top of the other in an offset manner, so that the metal-coordinated ligands sticking out of one layer will protrude into 50% of the interporphyrin voids of the inverted layer. The remaining pores are filled with a loosely packed (and orientationally disordered) second molecule of benzyl acetate. The water species incorporated into the lattice bridge between the uncoordinated benzyl-acetate and one of the OH sites of the metalloporphyrin. Translational displacement of such bilayered sections along the **b**-axis composes the entire structure. A nearly identical occlusion pattern has been observed in isomorphous crystals (triclinic, a = 13.423, b = 14.775, c = 15.181 Å, α = 81.78, β = 68.58, γ = 66.96°) containing the similarly shaped methyl phenylacetate guest ligand.

A similar type of layered interporphyrin arrangement has been observed in compound **15**, which also consists of 5-coordinate metalloporphyrin entities with a benzaldehyde moiety directly ligated to Zn at Zn•••O 2.22 Å (Fig. 8b). In this case, however, the structure is polar and all the porphyrin building blocks are oriented in the same direction, parallel to the screw-symmetry axis. The 5-coordinate porphyrins are located on crystallographic mirror planes. They form roughly planar two-dimensional H-bonded networks, aligned parallel to the (**ab**) plane of the crystal. Adjacent porphyrins associate directly through their *cis*-related hydroxyphenyl arms along **a**, and with the aid of an intervening water along **b**. These layers are stacked along the **c**-axis at equal intervals of c/4 with an offset geometry to allow the benzaldehyde ligands of one layer to protrude into the interporphyrin voids of the next array. The remaining interporphyrin voids in each layer and between layers are filled by a second molecule of benzaldehyde, located on and disordered about the mirror planes. Apparently, in the two structures of **14** and **15** there are no specific interactions other than dispersion between successive layers. A structurally characteristic feature in these compounds is the lock-and-key type fit between the axially coordinated ligand of one porphyrin layer and the interporphyrin pores of another layer.

Compound **16** is characterized by a somewhat different structure type. It contains only one-dimensional continuous arrays of nearly coplanar porphyrin molecules linked to one another by OH•••O hydrogen bonds between the *cis*-related hydroxyphenyl fragments of adjacent moieties (Fig. 9a). There are four molecules of acetophenone per each porphyrin. Two of them lie parallel to the planar porphyrin ring system above and below, their phenyl rings occupying the two axial ligating sites of the metal center. The other two molecules of the guest species approach the interporphyrin voids in each chain

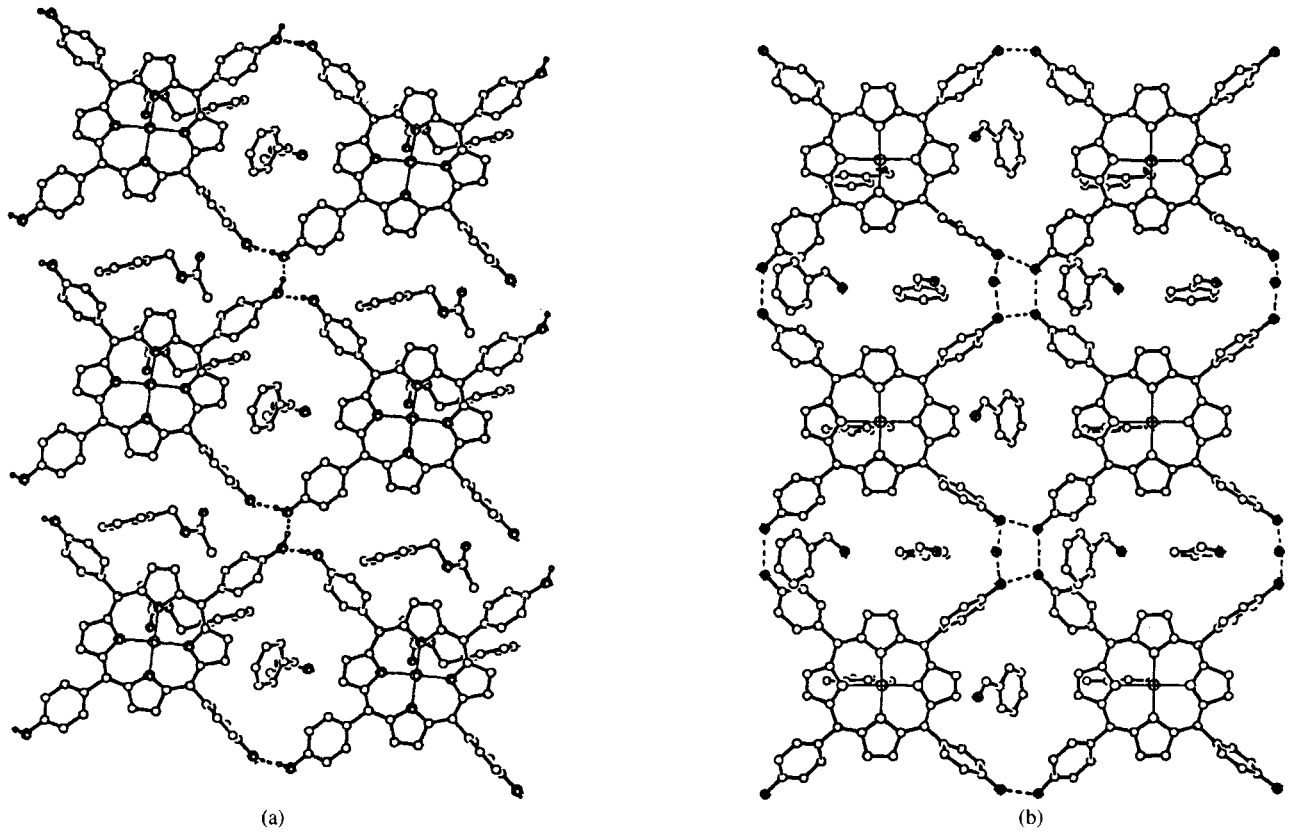

Figure 8 Illustration of the networked interporphyrin arrangement and accommodation of the guest ligands within interporphyrin pores in (a) **14**, and (b) **15**. It includes guests located behind and ligating to the metal centers of the porphyrins shown; guests having a parallel (in **15**) or antiparallel (in **14**) orientation coordinate to an adjacent porphyrin sheet (not included). The guest molecules not bound to the host framework can be recognized by their different orientation.

from opposite sides. The one-dimensional arrays are aligned parallel to one another in an offset manner, forming corrugated sheets similar to those observed in the triclinic structures of the unsubstituted tetraarylporphyrins [2,3]. The channels between them, extending in a direction parallel to the porphyrin plane, are occupied by double rows of the acetophenone guest species (Fig. 9b). Every second guest in each such row is weakly associated through π-π^* interactions to the metalloporphyrin core of an adjacent array. It provides also, however, a cross-linking feature to the structure by hydrogen-bonding through its carbonyl group to the OH-end of another row of metalloporphyrin molecules. The other differently oriented guest molecules are incorporated into the remaining interporphyrin voids. They are loosely packed and partly disordered, lacking any specific coordination to the surrounding entities.

Compound **17** (see Fig. 10) contains one-dimensional hydrogen-bonded porphyrin arrays very similar to the chain-motif seen in **16**. In this compound, however, the host lattice is based on six-coordinate metalloporphyrin complexes in which methanol molecules occupy the axial coordination sites (Zn•••O=2.459 Å). In addition to the methanol ligands, this material contains two non-ligated methanol molecules per porphyrin molecule. Hydrogen bonding between methanol molecules and the porphyrin hydroxyl groups cross-links the hydrogen-bonded chains into a three-dimensional network. Although the space groups and hydrogen bonding schemes of compounds **16** and **17** are different, the disposition of the *o*-xylene guest molecules in compound **17** are very similar to those of the acetophenone molecules in compound **16**.

Hydrogen bonded chains of the porphyrin molecules are also present in structure **18**. However, adjacent chains in this structure are interspaced by only a single row of the guaiacol molecules. Two of the guest species are contained between the overlapping chains. One is sandwiched between, and lies parallel to, the overlapping planar porphyrin cores, while the other is contained near the interporphyrin space of each chain. A new structural motif thus characterizes this structure, namely a columnar alternating arrangement of tightly overlapping face-to-face stacked fragments of an aryl group and a metalloporphyrin core (Fig. 11a). Additional molecules of the solvent are located in the interface between the stacked arrangements of the porphyrin chains. They hydrogen bond to the peripheral hydroxy groups of the porphyrins, and bridge between the neighboring porphyrin chains in each layered zone.

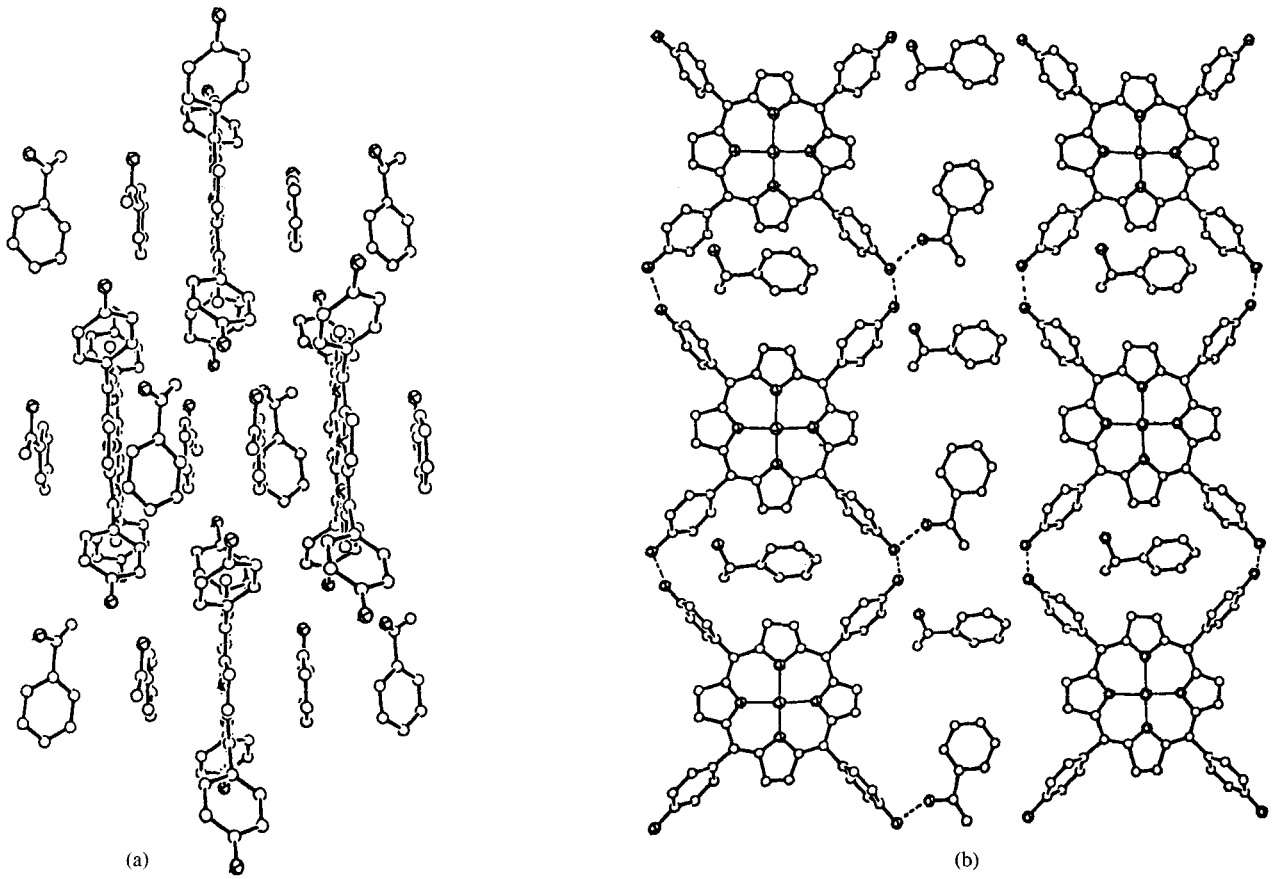

Figure 9 Two views of the intermolecular arrangement in **16**. Guest molecules lying parallel to the porphyrin core may weakly associate with the latter through charge-transfer π-π^* interactions. Guest molecules which hydrogen-bond to the hydroxyl ends of the porphyrin, as marked in (b), lie directly above the metalloporphyrin rings of an adjacent row of the porphyrin entities.

In an anhydrous aprotic nonpolar environment the 4-hydroxy-metalloporphyrin species forms a uniquely beautiful architecture (Fig. 11b). Thus, in compound **19** with no other polar species present in the bulk, all the hydroxyphenyl sites are utilized in interporphyrin H-bonding interactions. The resulting structure is characterized by high symmetry, the porphyrin moieties being located on 2/m sites and symmetrically linked to the surrounding molecules. The layered sections thus formed are stacked along the **b** axis in an overlapping manner. Successive layers, displaced by 6.5 Å, are interspaced by the planar molecules of the organic guest which are tightly enclosed between neighboring porphyrin cores. There are hydrogen bonds between the layers as well, inducing a strongly linked 3-dimensional lattice of the porphyrin moieties. The interporphyrin voids in the individual layers also overlap one another, forming channel-type pores in a perpendicular direction. The latter are accommodated by additional molecules of the organic guest. There is a considerable amount of guest disorder in the crystalline phase, and, therefore, atomic positions of the guest could not be located precisely. Guest molecules enclosed between the parallel metalloporphyrin rings and occupying the axial coordination sites of the metal ion are disordered orientationally in their molecular plane in the highly symmetric environment. Guests positioned in the channels are more free to move, and they exhibit a significant translational as well as rotational disorder.

All interporphyrin OH•••OH, porphyrin-OH•••water and porphyrin-OH•••methanol hydrogen bonds referred to above in this section are characterized by O•••O distances within the range 2.58–2.81 Å, representing strong interactions.

Structures of the Zn(II)-tetra-(4-chlorophenyl)porphyrins. This group of compounds also involves four-, five- and six-coordinate metalloporphyrin varieties. In structure **20**, the 4-coordinate host molecules are effectively packed in two-dimensional planar arrays. The interporphyrin arrangement is characterized by apparent Cl•••Cl interactions between the *cis*-related chlorophenyl arms of adjacent moieties, with the methyl phenylacetate guest being incorporated into the inter-host voids. Packing along the other direction is stabilized by electrostatic attraction between apposing C-Cl dipoles. This packing is further characterized by a perfect steric fit between the convex Cl•••Cl sites of one row of the porphyrins and the concave surface of an adjacent porphyrin

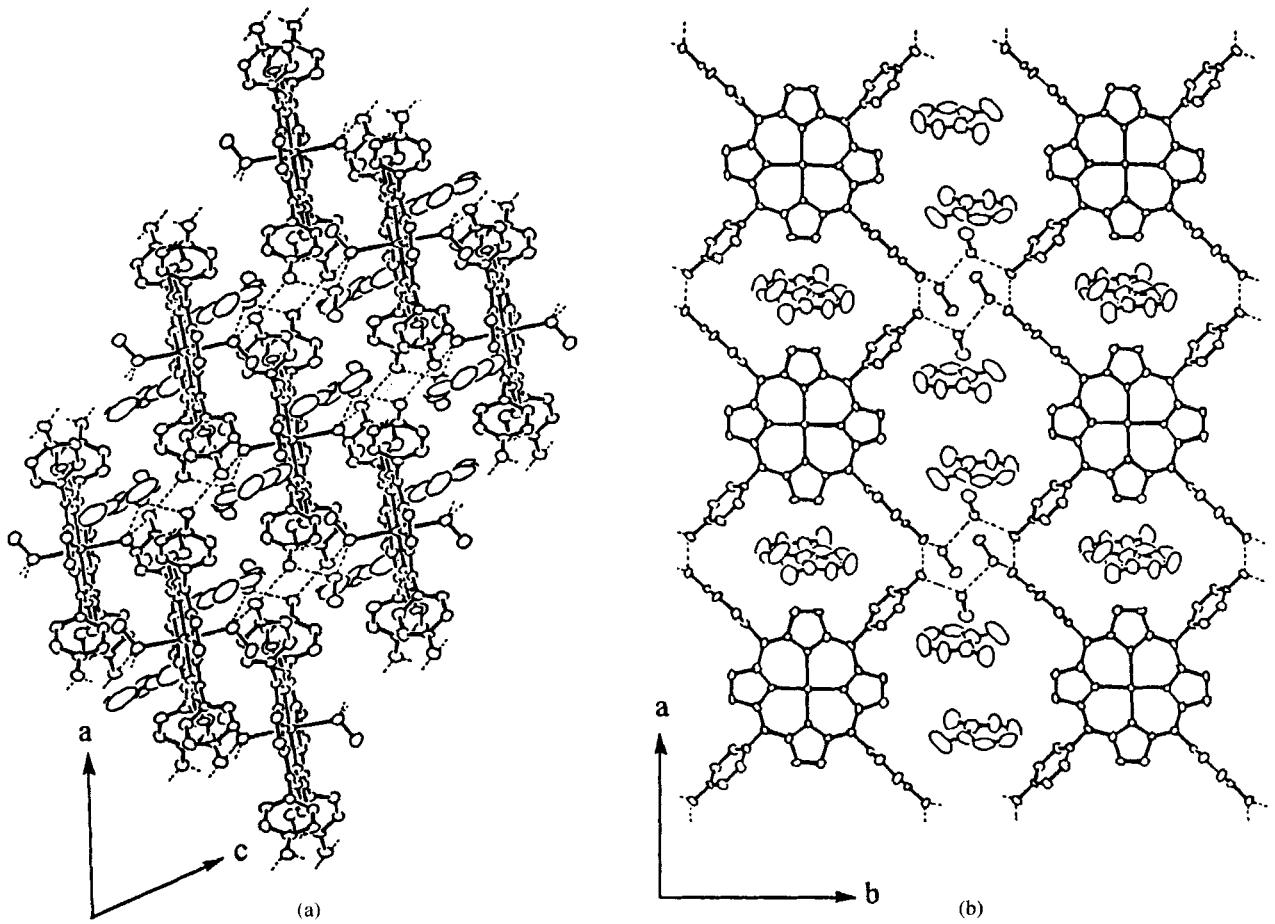

Figure 10 Two views of the packing arrangement in **17**. Dashed lines indicate the hydrogen bonding. (a) shows a projection down the **b** axis, and (b) shows a section parallel to the **ab** plane.

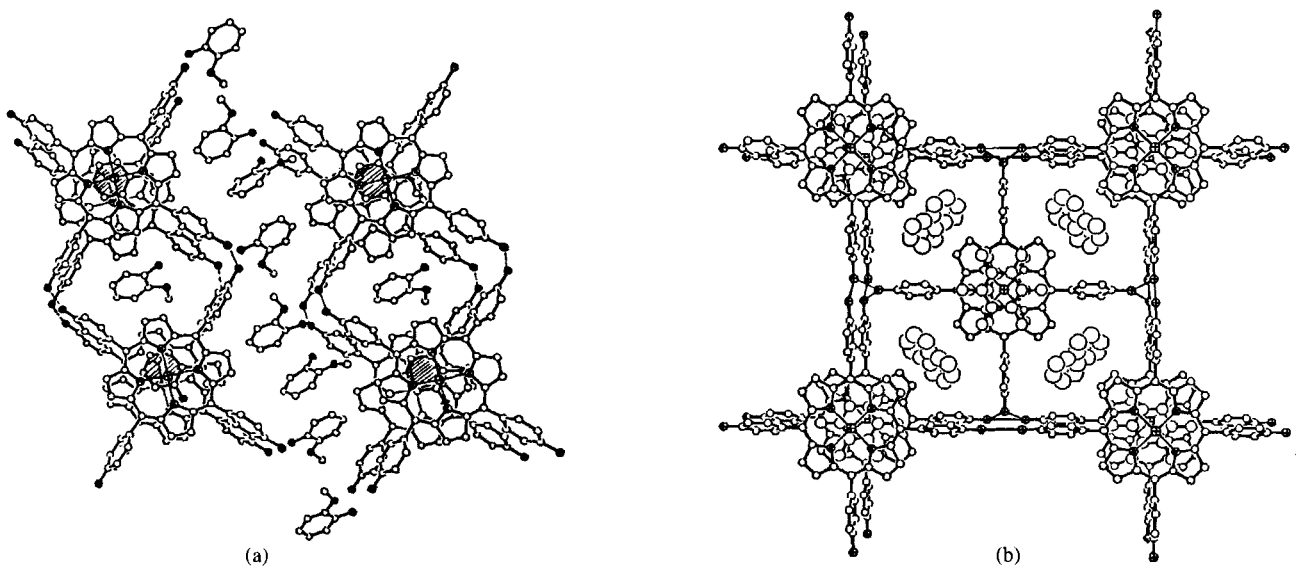

Figure 11 Illustration of the supramolecular arrangement in: (a) compound **18**, and (b) compound **19**, emphasizing the stacking motif in these structures. In (b), the guest entity intercollated between successive porphyrins in a stack is described by a hexamethylbenzene (an averaged representation of the solvent mixture of toluene, *o*-xylene, *m*-xylene and *p*-xylene probably contained in this lattice); that located in the interporphyrin channels (and translationally disordered as well) is represented by a naphthalene framework.

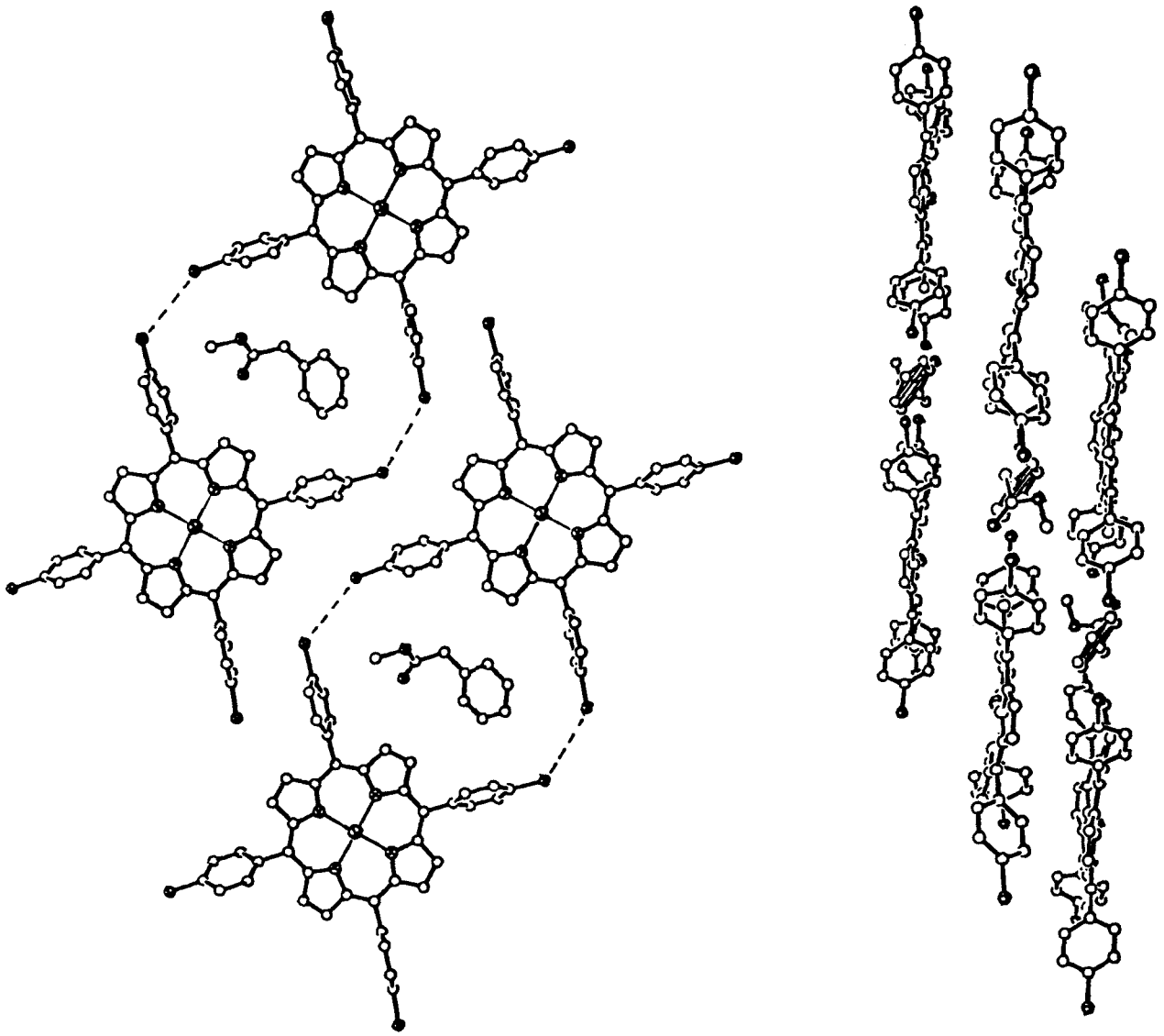

Figure 12 Two perspective views of **20**, showing incorporation of the guest species in the small interporphyrin voids. The dashed lines represent (also in Figures 12 – 15 below) apparent specific noncovalent interactions of the Cl•••Cl type.

row in a layer (Fig. 12). The layers are stacked along an axis normal to the porphyrin plane, without being interspaced by another species, but in an offset geometry. The proximity of neighboring layers causes a significant deformation from planarity of the porphyrin cores mainly due to steric hindrance between the aryl substituents of one layer and the porphyrin core of another (the two rings are nearly perpendicular to one another).

The same characteristic layered pattern of the porphyrins, incorporating small organic moieties, occurs also in compound **21**. In this case, molecules of apolar mesitylene are incorporated into the interhost cavities. However, the planar sections are arranged this time in an almost overlapping manner along the stacking direction (Fig. 13). Correspondingly, the interporphyrin sites of each layer are located one on top of the other, thus combining to a continuous channel-type cavity filled by the organic guest. The latter, lacking specific interactions with the channel walls have a considerable freedom of motion along these channels, and are translationally disordered. Careful inspection of difference electron-density maps and data from DSC/TGA measurements revealed that water molecules (in a nonstoichiometric ratio, see Table 1) are also trapped in these channels in a disordered manner. As a further result of the face-to-face stacking, the porphyrin cores are distorted from planarity, as in the previous example. Isomorphous arrangements appear to occur also in the crystalline complexes of **5** with other organic moieties, including toluene, anisole, and *o*-chlorophenol.

Compound **22**, although consisting of a 5-coordinate metalloporphyrin moiety, exhibits a similarly layered arrangement, with Cl•••Cl interactions in one direction and dipole-dipole attractions in the other. However, this

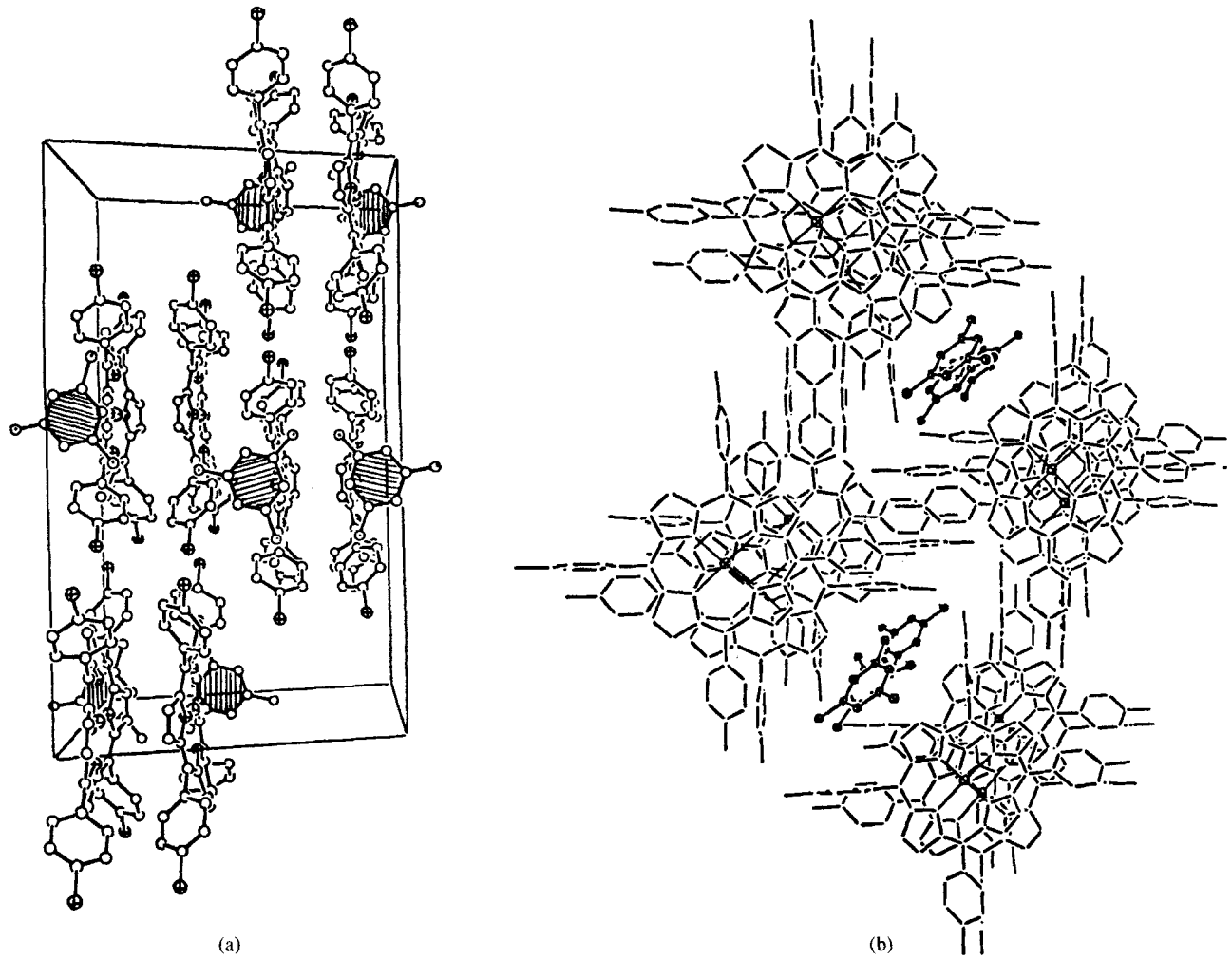

Figure 13 Illustration of the intermolecular arrangement in **21**, showing the columnar stacking of the chlorophenyl-porphyrins, and the guest (mesitylene) inclusion in the interporphyrin channels. The structure of the guest is incommensurate with the porphyrin host lattice, and could not be defined precisely. (a) View perpendicular to the channel axis, with the guest species (shown at selected sites) shaded for clarity. (b) View approximately down the channel axis.

structure is polar and all the layers are oriented in the same direction. Stacking of the layered sections is such that the metal-coordinated ethylbenzoate ligand of one layer is inserted into the interporphyrin pores of another layer. This key-to-lock type steric complementarity yields an effectively packed crystal structure (Fig. 14).

The above described packing modes are further modified for 6-coordinate metalloporphyrin compounds. Thus, structure **23** also contains rows of the porphyrin entities which link to one another through the Cl•••Cl noncovalent interactions between the *cis*-related chlorophenyl arms of adjacent species. In a stack of such rows, the two metal-ligating acetophenones (at C = O•••Zn distances of 2.69 Å) of one entity protrude into and effectively fill the interporphyrin voids of the neighboring rows located above and below. Sideways, adjacent sheets of stacked rows of the 6-coordinate entities interlock effectively, by complementary arrangement of their convex and concave surfaces in order to optimize the electrostatic attractions between them *via* interactions between their chlorophenyl fragments. The resulting structure (Fig. 15) can thus also be described as consisting of corrugated sheets of tightly arranged porphyrin moieties, interlinked by the Cl•••Cl contacts. These sheets are interspaced by zones of the organic guest molecules.

Finally, the crystal packing of compound **24**, involving again a 4-coordinate moiety, resembles to a considerable extent the structural form previously observed for the 4-methoxyphenyl-metalloporphyrin derivative (see above). Thus, the porphyrin entities, stacked in an offset manner, form tightly packed sheets of parallel molecular units. Each porphyrin core is approached from above and below by two pairs of opposed chlorophenyl groups of the neighboring porphyrin species. Packing of these sheets, which is also stabilized by dipolar attractions between the other chlorophenyl fragments, is less effective, leaving voids accommodated by molecules of nitrobenzene.

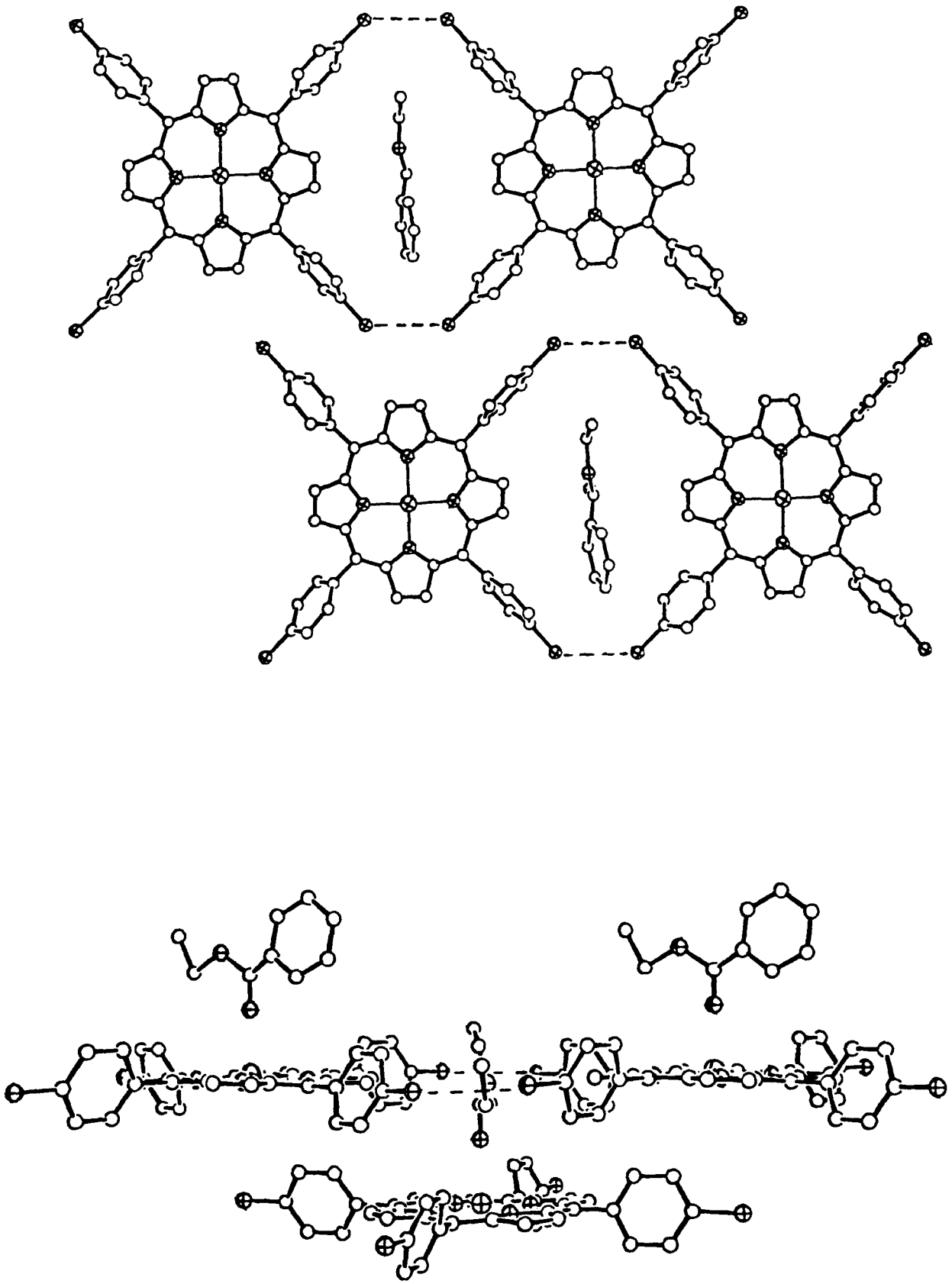

Figure 14 Two perspective views of the packing arrangement in **22**. Note the lock-and-key type fit between neighboring layers of the **5**-coordinate porphyrin entities, and the perfect occlusion of the guest between the chlorophenyl arms of adjacent hosts.

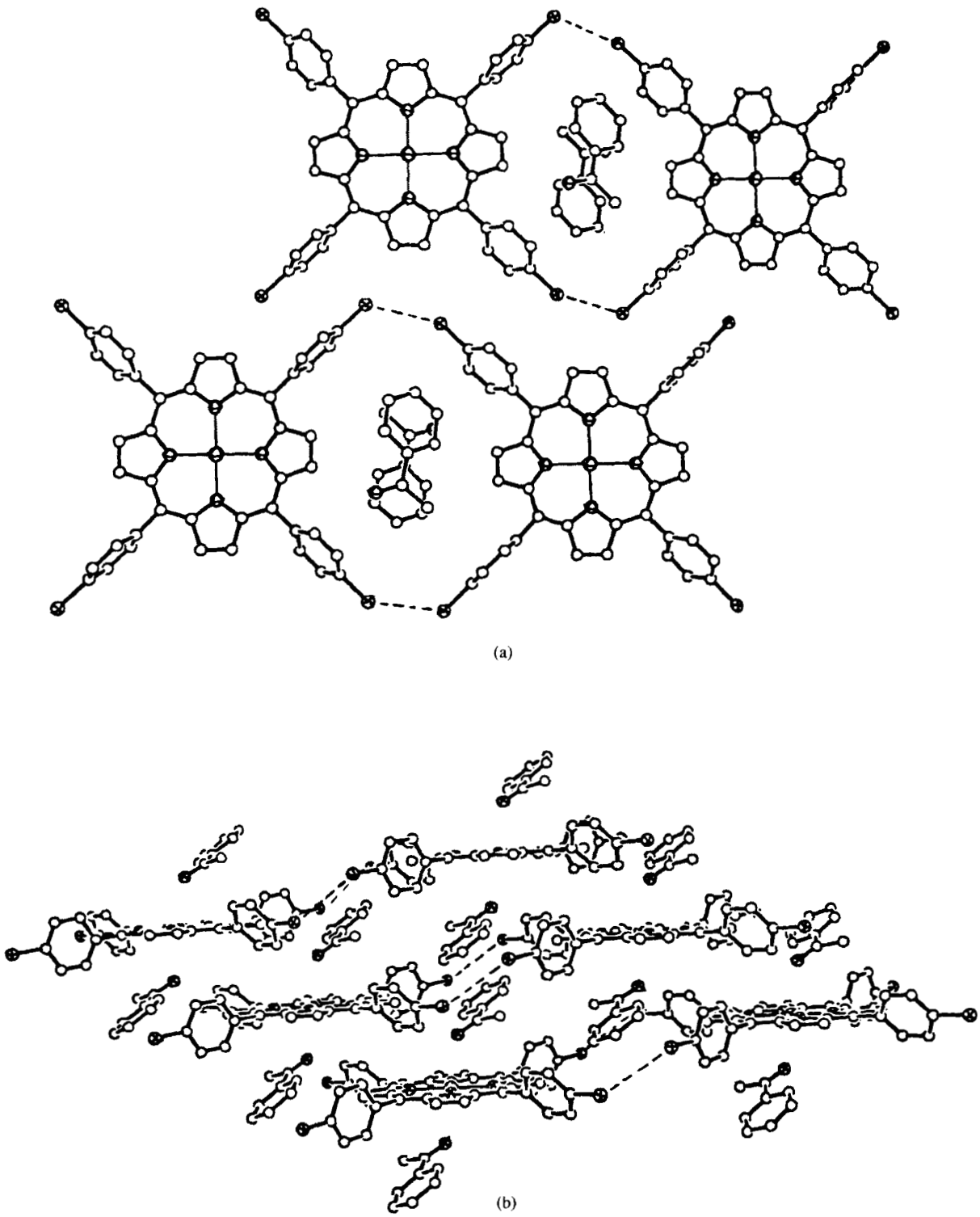

Figure 15 Crystal packing in **23**. Views: (a) on the porphyrin plane, and (b) parallel to the porphyrin plane.

The characteristic Cl•••Cl dipolar attractions are also utilized to enforce the porphyrin lattice. However, in this case a helical (rather than planar) pattern of the Cl•••Cl interactions is formed around every guest site, linking between a porphyrin species in one sheet with two porphyrin entities displaced by **b** of an adjacent sheet. Such an arrangement yields a polarized cavity environment between the porphyrin building blocks, enhancing a polar alignement of dipolar organic species along the interporphyrin voids (Fig. 16).

The average Cl•••Cl nonbonding contacts between the *cis*-related chlorophenyl arms of adjacent porphyrin

moieties in the above structures are 3.8 Å in **21**, **22** and **23**, 4.0 Å in **20** and 4.1 Å in **24**. Although they cluster in the higher range of Cl•••Cl distances still indicative of specific interaction, [18,19] the common appearance of the geometric patterns observed for **20–23**, and the similarity of the basic structural "chain" motif to that found in the H-bonded hydroxyphenyl derivatives, suggest their significance in the presently analysed crystals as well. In all of these structures the neighboring C-Cl bonds approach one another roughly at right angles.

DISCUSSION

The structural data obtained for the 4-methoxy substituted compounds reveal some interesting details. They confirm that the tetraphenylporphyrin molecular framework, with the four aryl rings nearly perpendicular to the porphyrin core, can pack tightly only in two dimensions. The less effective arrangement along the third axis provides a driving force for a co-crystallization process with guest species from the solvent in order to fill the intermolecular pores between the porphyrin layers. In this respect, compounds **6–8** represent clathrate-type structures.

The methoxy substituent is a weak functional group of low polarity, which can be utilized in directional intermolecular interactions only in the presence of protic polar functions. In the absence of the latter, the dominant effect of the molecular shape on crystalline packing is similar for the methoxy-substituted and the unsubstituted tetraphenylporphyrin derivatives. The packing efficiency of the porphyrin host compounds varies, however, in direction between the 4-coordinated and the 6-coordinated materials. Thus, in compounds **6–8** the porphyrins pack densely along a direction perpendicular to the porphyrin plane, while in **10** they pack well in directions parallel to the molecular plane. In the latter case the porphyrins arrange in corrugated sheets, which are interspaced by the weakly bound axial (with respect to the metal coordination) ligands.

The structure type of the 5-coordinate material **9** resembles that observed for the 4-coordinate clathrates **6–8**. However, in **9** the interporphyrin arrangement with-

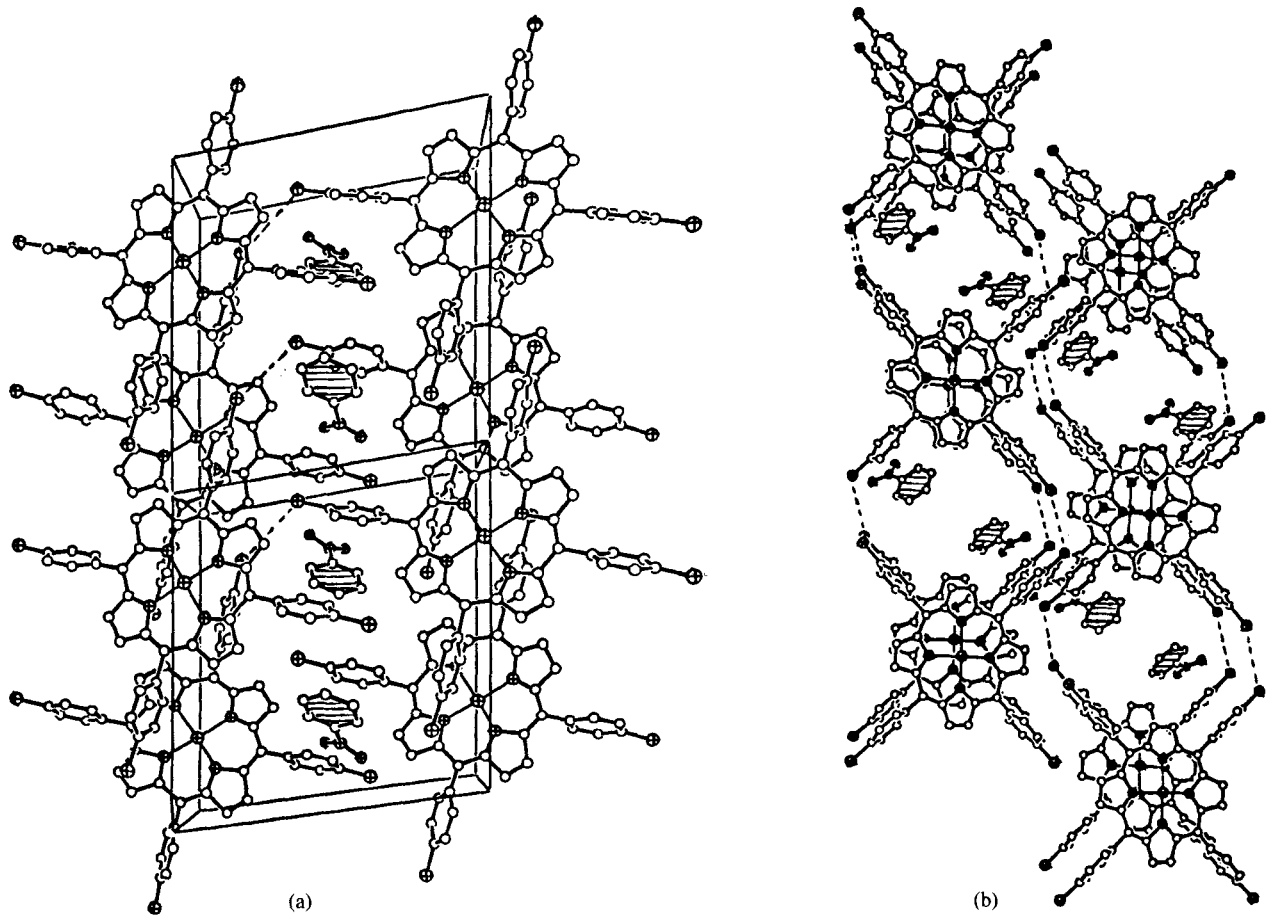

Figure 16 (a) The crystal structure of **24**, viewed down the **b**-axis, showing the dipolar alignement of nitrobenzene in voids between layers of stacked porphyrin moieties. Two unit-cells are shown. (b) View of the helical arrangement of the Cl•••Cl interactions, creating a polarized environment for guest molecules incorporated into the lattice. The overlapping porphyrins shown are displaced by a unit-cell translation along **b**.

in the layer is expanded to allow for a stronger association between adjacent units of the 5-coordinate metalloporphyrin complex through H_2O•••OMe hydrogen bonds. This illustrates the significant role that the porphyrin metal center can play in affecting the nature of the intermolecular association. A suitable reagent (exemplified by water in **9**) can simultaneously be bound to the metal of one porphyrin species and to a peripheral sensor group of an adjacent porphyrin molecule, thus incorporating cross-links and rigidity into the layered arrangement of the porphyrin moieties. These features are similar, to an extent, to the cofacial assembly of metallophthalocyanine, through axially positioned hydroxy ligands, in the form of crystalline polymers [20].

Introduction of the hydroxyl groups onto the phenyl rings introduces diverse options of intermolecular interaction. The OH group functions as a proton donor as well as a proton acceptor, and can play an important role in determining the geometry of intermolecular organization [21]. The nature of the crystallization medium may also have a significant effect on the structure which forms. In particular, there is a striking difference between crystals grown from solvent mixtures with a relatively high water content and those obtained from polar and nonpolar aprotic solvents. Water provides a hydration shell to the hydroxy groups of the porphyrin hosts, thus reducing their effectiveness in the formation of porphyrin-porphyrin linkages. Moreover, as shown in **9** molecules of water can coordinate to the metal center, and serve an intermolecular cross-linking function competetive to that of the OH group. These features are well illustrated by structures **11**–**13** (representing 4-coordinate as well as 5-coordinate metalloporphyrin complexes) in which the major solvating and ligating role of water is clearly evident.

The most common mode of H-bond assisted assembling of the porphyrin host is revealed, however, in structures **13**–**18**, in which the hosts associate through the *cis*-related hydroxyphenyl residues of neighboring moieties. The basic motif is a continuous one-dimensional 'polymer' of linked porphyrin species. In some cases the porphyrin arrays are sufficiently close to afford direct interporphyrin H-bridges between the chains in a perpendicular direction as well. This leads to the formation of either two-dimensional (in **14** and **15**) or with nonpolar aprotic guests even three-dimensional (in **18**) aggregates of the porphyrins. The hollow architecture of these motifs may be characterized by the largest van der Waals dimension of the interporphyrin cavity of about 9Å (the distance between the two OH•••OH linkages, less 3Å), being perfectly suited for a favorable occlusion of stoichiometric amounts of small molecular entities. Occurence of the interlinked porphyrin motif appears to be little dependent on space symmetry, the nature of the ligand, and on whether the interaction of the latter with the porphyrin core is of coordination, or molecular complex formation, type.

An additional variant of structures **14**–**18** is the type of stacking between parallel chains or layers of the porphyrin hosts. In materials **14**–**16** the hydrogen-bonded porphyrin motifs are stacked in an offset manner, and there is no overlap between the interporphyrin cavities of adjacent arrays. Thus, the host-bound as well as the unbound guest molecules are aligned in channel-type zones which extend parallel to the porphyrin plane between adjacent networks of the porphyrin species. A particularly clear illustration of this pattern can be seen in Fig. 9 depicting the crystal structure of compound **16**.

In compounds in which the interaction of the guest molecules with the metalloporphyrin core is primarily of the π-π^* charge-transfer type, an almost fully overlapping arrangement of the adjacent porphyrin chains or layers is enforced in the crystal. This is demonstrated by compounds **17** and **18** in which a single guest molecule (guaiacol or toluene) is tightly intercollated between two overlapping porphyrin ring systems (Fig. 10). The corresponding crystals thus consist of CT-stabilized columns of alternating metalloporphyrin and guest moieties. These columns are strongly linked to one another *via* hydrogen bonds in direction(s) perpendicular to the column. Successive interporphyrin cages, which combine now into a channel type structure, are occupied (as in the previous examples) by a second group of uncoordinated guest molecules. The rate at which a guest molecule diffuses through these channels will depend on its shape and size.

The above examples indicate that the offset geometry between the porphyrin layers in the crystal and the channel architecture can be controlled to a reasonable extent by the nature of the guest constituent. Polar ligands with strong nucleophilic sites (such as the carbonyl group, or water) capable of forming coordinative bonds to the metal center, will favor a non-overlapping arrangement of the porphyrin chains, while aromatic components involved in charge-transfer interactions with the metalloporphyrin ring are better fit to induce a face-to-face stacking geometry. The latter architecture, as demonstrated ideally by the structure of **18**, resembles the structural rigidity of a zeolite. The metalloporphyrin building blocks are effectively interconnected in the solid in three dimensions, and form a stable and rigid lattice with a well defined channel structure.

Compounds based on the chlorosubstituted porphyrins were found to form similarly networked structural modes, in which the OH•••OH hydrogen bonds are replaced by Cl•••Cl contacts. It appears that the halogen-halogen interactions are strong enough to direct formation of extended host networks by optimization of the Cl•••Cl interactions between neighboring host entities. Since typically the Cl•••Cl contacts are longer by about 1

Å than the OH•••OH hydrogen bonds, the interporphyrin cavities in the chlorophenyl compounds are slightly larger than in the hydroxyphenyl materials, allowing for a more effective occlusion of the guest components in these voids. Characteristic arrangements are illustrated in Figs. 11–14. These structures (**19–22**) contain continuous chains of interlinked porphyrin moieties, which are arranged in layers by tightly fitting the convex surfaces of one chain into the concave surfaces of adjacent chains. In all cases the guest or ligand molecules are confined within or located near the interporphyrin voids. A genuine channel type architecture has been observed only in compound **20** involving an aromatic nonpolar guest as mesitylene. The beautifully crystalline material first isolated from the corresponding solution was observed to deteriorate gradually due to the guest free motion along, and eventual release from, the channels.

The last structure type referred to in this study, **23**, is unique in the sense that it contains a polar axis, and exhibits a dipolar alignment of the occluded and uncoordinated guest component (nitrobenzene) along this axis. The nitrobenzene molecules are incorporated into the interporphyrin voids, and are surrounded by a helical arrangement of the Cl•••Cl interactions. Consequently, this arrangement is associated with the formation of a large bulk dipole moment in the crystal, a potentially important feature in the design of composite solids with nonlinear optical properties based, for example, on reduced porphyrin systems.

It has been shown in this study that functionalization of the tetraphenylporphyrin framework by OH and Cl substituents has a significant effect on the crystal packing modes of the metalloporphyrin species. The microstructure of these compounds (including the size of the intermolecular pores) is determined not only by the molecular shape of the rigid bulky porphyrin system, but also by specific noncovalent bonds which fine-tune the intermolecular architecture. In this respect, it is of little importance whether the produced materials can formally be classified as clathrates, coordination compounds or molecular complexes. Formation of these heteromolecular materials, *via* guest/ligand extraction from the solution and crystallization, followed the same experimental procedure irrespective of the compound type. The different kinds of intermolecular host (porphyrin)-guest (ligand/solvent) interactions involved may influence the stability of the composite material and the dynamics of the guest included in it, and thus provide degrees of freedom to control these properties.

The networked aggregation of the functionalized porphyrin building blocks and the hollow architecture of the aggregates are features common to microporous solid materials utilized in storage and transport of molecules and ions. Evaluation of the thermodynamic and kinetic properties of some of the above solids is, therefore, of a particular interest. Structural investigations of other materials consisting of tetra-4-carboxyphenyl, tetra-4-pyridyl, and tetra-3-hydroxyphenyl derivatives of the porphyrin building blocks, which may reveal different structural characteristics of guest incorporation, are also in progress, and will be discussed elsewhere.

ACKNOWLEDGMENTS

This research was supported in part by grant No. 90-00061 from the United States-Israel Binational Science Foundation (BSF), Jerusalem, Israel.

REFERENCES AND NOTES.

1 Scheidt, W. R.; and Lee, Y .J., *Struct. Bond. (Berlin)*, **1987**, *64*, 1.
2 Byrn, M. P.; Curtis, C. J.; Khan, S. I.; Sawin, P. A.; Tsurumi, R. and Strouse, C. E., *J. Am. Chem. Soc.*, **1990**, *112*, 1865.
3 Byrn, M. P.; Curtis, C. J.; Goldberg, I.; Hsiou, Y.; Khan, S. I.; Sawin, P. A.; Tendick, S. K. and Strouse, C. E., *J. Am. Chem. Soc.*, **1991**, *113*, 6549.
4 Byrn, M. P.; Curtis, C. J.; Hsiou, Y.; Khan, S. I.; Sawin, P. A.; Tendick, S. K.; Terzis, A. and Strouse, C. E., *J. Am. Chem. Soc.*, **1993**, *115*, 9480.
5 Schick, G. A.; Schreiman, I. C.; Wagner, R. W.; Lindsey, J. S. and Bocian, D.F., *J. Am. Chem. Soc.*, **1989**, *111*, 1344.
6 Imai, H., Nakagawa, S. and Kyuno, E. *J. Am. Chem. Soc.* **1992**, *114*, 6719.
7 Aoyama, Y.; Asakawa, M.; Matsui, Y. and Ogoshi, H., *J. Am. Chem. Soc.*, **1991**, *113*, 6223.
8 Danks, I. P.; Sutherland, I. O.; and Yap, C. H., *J. Chem. Soc., Perkin Trans.*, **1990**, *1*, 421.
9 Some preliminary results of this investigation have been published in: Byrn, M. P.; Curtis, C. J.; Goldberg, I., Huang, T., Hsiou, Y., Khan, S. I.; Sawin, P. A.; Tendick, S. K.; Terzis, A. and Strouse, C. E., *Mol. Cryst. Liq. Cryst.*, **1992**, *211*, 135, as well as in references 2 and 3.
10 Tecilla, P., Dixon, R. P.; Slobodkin, G.; Alavi, D. S.; Waldeck, D. H. and Hamilton A. D., *J. Am. Chem. Soc.*, **1990**, *112*, 9408.
11 Suslick, K. S.; Chen, C.-T.; Meredith, G. R. and Cheng, L.-T., *J. Am. Chem. Soc.*, **1992**, *114*, 6928.
12 Golder, A. G.; Nolan, K. B.; Povey, D. C.; Milgram, L. R., *Acta Crystallogr.*, **1988**, *C44*, 1916.
13 Golder, A. G.; Nolan, K. B.; Povey, D. C.; Traylor, T. Q., *Inorg. Chim. Acta*, **1988**, *143*, 71.
14 Main, P.; Fiske, S. J.; Hull, S. E.; Lessinger, L.; Germain, G. Declercq, J. P. and Woolfson, M. M., MULTAN 80. *A System of Computer Programs for the Automatic Solution of Crystal Structures from X-Ray Diffraction Data*, University of York, England, **1980**.
15 Sheldrick, G. M., SHELX 86, in *Crystallographic Computing 3*, eds. G.M. Sheldrick, C. Kruger, and R. Goddard, Oxford University Press, pp. 175–189, **1985**.
16 Sheldrick, G. M., SHELX 76, *A Program for Crystal Structure Determination*, University of Cambridge, England, **1976**.
17 Munro, O. Q.; Bradley, J. C.; Hancock, R. D.; Marques, H. M.; Marsicano F. and Wade P. W., *J. Am. Chem. Soc.*, **1992**, *114*, 7218.
18 Desiraju, G. R., in *Organic Solid State Chemistry*, ed. G.R. Desiraju, Elsevier, pp. 519–546, **1987**.
19 Weber, E.; Dorpinghaus, N.; Wimmer, C.; Stein, Z.; Krupitsky, H.; and Goldberg, I., *J. Org. Chem.*, **1992**, *57*, 6825.
20 Marks, T. J., *Angew. Chem., Int. Ed. Engl.*, **1990**, *29*, 857, and references cited therein.
21 Etter, M.C., *J. Phys. Chem.*, **1991**, *95*, 4601, and references cited therein.